FI SEVIER

Contents lists available at ScienceDirect

### European Journal of Medicinal Chemistry

journal homepage: http://www.elsevier.com/locate/ejmech



### Research paper

# Expanding the anticancer potential of 1,2,3-triazoles via simultaneously targeting Cyclooxygenase-2, 15-lipoxygenase and tumor-associated carbonic anhydrases



Perihan A. Elzahhar <sup>a, \*, 1</sup>, Shrouk M. Abd El Wahab <sup>b, 1</sup>, Mohamed Elagawany <sup>b, c</sup>, Hoda Daabees <sup>b</sup>, Ahmed S.F. Belal <sup>a</sup>, Ahmed F. EL-Yazbi <sup>d, e</sup>, Ali H. Eid <sup>e</sup>, Rana Alaaeddine <sup>e</sup>, Rehab R. Hegazy <sup>f</sup>, Rasha M. Allam <sup>f</sup>, Maged W. Helmy <sup>g</sup>, Bahaa Elgendy <sup>c</sup>, Andrea Angeli <sup>h</sup>, Soad A. El-Hawash <sup>a, \*\*</sup>, Claudiu T. Supuran <sup>h, \*\*\*</sup>

- <sup>a</sup> Department of Pharmaceutical Chemistry, Faculty of Pharmacy, Alexandria University, Alexandria, 21521, Egypt
- <sup>b</sup> Department of Pharmaceutical Chemistry, Faculty of Pharmacy, Damanhour University, Damanhour, 22516, Egypt
- <sup>c</sup> Center for Clinical Pharmacology, Washington University School of Medicine and St. Louis College of Pharmacy, St. Louis, MO, 63110, USA
- <sup>d</sup> Department of Pharmacology and Toxicology, Faculty of Pharmacy, Alexandria University, Alexandria, 21521, Egypt
- e Department of Pharmacology and Toxicology, Faculty of Medicine, The American University of Beirut, Beirut, Lebanon
- f Department of Pharmacology, Medical Division, National Research Centre, Giza, Egypt
- g Department of Pharmacology & Toxicology, Faculty of Pharmacy, Damanhour University, Damanhour, 22516, Egypt
- h Universita, Degli Studi di Firenze, NEUROFARBA Dept, Sezione di Scienze Farmaceutiche, Via Ugo Schiff 6, 50019, Sesto Fiorentino, Florence, Italy

### ARTICLE INFO

Article history: Received 14 December 2019 Received in revised form 5 May 2020 Accepted 6 May 2020 Available online 25 May 2020

Keywords: Cancer 1,2,3-Triazoles MTDL Cyclooxygenase-2 15-Lipoxygenase Carbonic anhydrase Apoptosis

### ABSTRACT

Cancer is a multifactorial disorder involving multiplicity of interrelated signaling pathways and molecular targets. To that end, a multi-target design strategy was adopted to develop some 1,2,3-triazoles hybridized with some pharmacophoric anticancer fragments, as first-in-class simultaneous inhibitors of COX-2, 15-LOX and tumor associated carbonic anhydrase enzymes. Results revealed that compounds 5a, 5d, 8b and 8c were potent inhibitors of COX-2 and 15-LOX enzymes. COX-2 inhibitory activity was further demonstrated by the inhibition of the accumulation of 6-keto-PGF1α, a metabolite of COX-2 products in two cancer cell lines. The sulfonamide bearing derivatives 5d and 8c were effective nanomolar and submicromolar inhibitors of tumor associated hCA XII isoform, respectively. Strong to moderate inhibitory activities were observed in the in vitro antiproliferative assay on lung (A549), liver (HepG2) and breast (MCF7) cancer cell lines (IC<sub>50</sub> 2.37–28.5 µM) with high safety margins on WI-38 cells. A cytotoxic advantage of CA inhibition was observed as an increased activity against tumor cell lines expressing CA IX/XII. Further mechanistic clues for the anticancer activities of compound 5a and its sulfonamide analog 5d were derived from induction of cell cycle arrest at G2/M phase. They also triggered apoptosis via increasing expression levels of caspase-9 and Bax together with suppressing that of Bcl-2. The *in vitro* anti-tumor activity was reflected as reduced tumor size upon treatment with **8c** in an in vivo cancer xenograft model. Docking experiments on the target enzymes supported their in vitro data and served as further molecular evidence. In silico calculations and ligand efficiency indices were promising. In light of these data, such series could offer new structural insights into the understanding and development of multi-target COX-2/15-LOX/hCA inhibitors for anticancer outcomes.

© 2020 Elsevier Masson SAS. All rights reserved.

### \* Corresponding author.

E-mail addresses: perihan.elzahhar@alexu.edu.eg (P.A. Elzahhar), soad. elhawash@alexu.edu.eg (S.A. El-Hawash), claudiu.supuran@unifi.it (C.T. Supuran).

### 1. Introduction

Tumor-related inflammation has been clearly acknowledged as one of the hallmarks of cancer [1]. The association between inflammation and tumor progression was dated back to the nineteenth century when first observed by Virchow and has been

<sup>\*\*</sup> Corresponding author.

<sup>\*\*\*</sup> Corresponding author.

<sup>&</sup>lt;sup>1</sup> These authors contributed equally to this work.

recently supported by many genetic and epidemiological studies [2]. As a matter of fact, the majority of precancerous and cancerous tissues are abundant in innate immune cells and inflammatory mediators such as chemokines and cytokines [3]. Both immune cells and inflammatory mediators influence different stages of tumor growth, starting from tumor initiation till metastasis [4]. Around 20% of cancer deaths are correlated to inflammation and chronic infections as exemplified by inflammatory bowel diseases, bronchitis and prostatitis [2]. Interestingly, the genetic stability of most of the cell types engaged in cancer-associated inflammation has been the focus of many anticancer drug design programs, owing to the decreased likelihood of rapid development of drug resistance [5].

In addition to their key role in inflammation and tissue homeostasis, eicosanoids, produced from arachidonic acid metabolism, have been implicated in the pathophysiology of cancer [2]. Cyclooxygenases (COX-1/2) and lipoxygenases (5/8/12/15-LOX) are among the major enzymes involved in the formation of eicosanoids [2].

COX-2 plays a crucial role in oncogenesis [2], whereby it contributes to initiation of cancers, promotion of angiogenesis and downregulation of apoptosis [6]. Increased COX-2 expression levels were experienced with human colorectal cancer and mouse models of adenomas [7], as well as a wide range of cancers such as breast, prostate, pancreatic cancers, esophageal, lung carcinomas and melanoma [2]. For this reason, several research groups thoroughly investigated the anticancer potential of selective COX-2 inhibitors in inflammation-related experimental tumor models [2]. Besides, the anticancer activity of some conventional chemotherapeutic agents and radiation was potentiated by the use of celecoxib [8,9]. Also, COX-2 inhibitors demonstrated potential to overcome multidrug resistance via reducing the expression of some efflux pumps, adding a new dimension to their therapeutic utility [6].

The second pathway comprises lipoxygenases which exist in humans mainly as 3 different isozymes; 5-LOX, 12-LOX, and 15-LOX (present in at least 2 isoforms 15-LOX-1 and 15-LOX-2) [2]. The complex interplay among LOX enzymes and their AA metabolites in tumor microenvironment has been clearly described in many reports [2,10,11]. Although 15-LOX seems to be pro-tumorigenic and antitumorigenic depending on the tissue [2,10], the selective 15-LOX inhibitor, PD146176, showed antiproliferative activity against prostatic cancer cells [11]. In addition, most reports targeting eicosanoids for anticancer effects focused on dual COX-2/LOX inhibition [2,12–15]. These inhibitors proved to be superior to their corresponding single pathway inhibitors [16]. This follows the premise that suppressing only COX-2 branch, would shift the AA metabolic machinery towards excessive production of LOX downstream inflammatory mediators and hence aggravate the incidence of side effects [16].

Apart from eicosanoids, carbonic anhydrases (CAs) represent a superfamily of zinc metalloenzymes that are widely spread in all living organisms. Seven distinct genes families encode CAs of which sixteen  $\alpha$ CA isozymes have been characterized *hitherto* in humans [17]. Of particular interest to this study, hCA IX and XII have been linked to tumors and some of their inhibitors are in clinical trials as anticancer and antimetastatic agents [18].

Hence, in seeking multi-targeting directed ligands (MTDLs) for future application as anticancer agents and probes, we herein report the design and synthesis of first-in class MTDLs as potential simultaneous COX2/15-LOX as well as carbonic anhydrase inhibitors. It is noteworthy that, combining activities towards two (out of three) of the selected targets have been previously attempted [19]. Indeed, the anti-tumor properties of celecoxib were attributed, at least partially, to hCA inhibitory activity in addition to COX-2 inhibition [20]. Moreover, some dual COX-2/hCA inhibitors

were designed for potential anti-tumor and anti-inflammatory effects [17,19]. Also, we successfully designed dual COX-2/15-LOX inhibitors, either acting merely on these two targets [21] or acting on additional targets within complex inflammatory disorders, such as Alzheimer's [22] and diabetes [23].

Consequently, we adopted a pharmacophoric hybridization strategy to modulate these structurally distinct targets. Our assembly relied on 1.2.3-triazole as the main scaffold by virtue of its recognized anticancer properties [24] as well as COX-2 and 15-LOX inhibitory activities, featured by our anti-inflammatory endeavors [21-23] (Fig. 1, Structure A). Also, a sulfonamide-incorporating 1,2,3-triazole showed tumor-associated hCA inhibitory activity [18] (Fig. 1, Structure B). We also envisaged incorporating the bioactive (thio)semicarbazone [25], thiazole [26] and pyrazole [14] pharmacophoric elements, at position-4 of the 1,2,3-triazole either directly or through a linker. They were selected on account of their contribution to some previously reported anticancer lead compounds (Structures C [25], D [26] and E [14], respectively). Therefore, three target structures were designed, based on the 1,2,3triazole anchoring an aryl moiety at position-1. Para position of the latter was substituted with some electron-withdrawing groups, including CA zinc binders [27].

Our rationale of triple targeting of COX-2, 15-LOX and carbonic anhydrase is very relevant, and in fact, might extend the scope of the current anticancer MTDL toolbox. This is due to the fact that complex pathological conditions, such as cancer, are characterized by interrelated pathways along with redundancies, compensatory mechanisms and development of drug resistance [28]. Hence, using the "one-molecule-one-target" approach in such complicated scenarios turned out to be unproductive and even counterproductive in many instances [29]. As a matter of fact, MTDLs have manifested themselves as bona fide tools for the management of multifactorial diseases such as cancer [28]. Additionally, a recent report confirmed the interplay between level of expression of COX-2 and carbonic anhydrase IX within colorectal cancer [30]. However, the exact molecular details underlying this interplay is not fully elucidated [30,31]. Hence, compounds targeting both arachidonate and carbonic anhydrase pathways can be used as probes to provide more insights and better understanding of this interplay. To conclude, the outcome of this study might help in both combating and expanding our knowledge of this disease.

Accordingly, we present the synthesis of the designed ligands along with their *in vitro* COX-2/15-LOX inhibitory activities. In addition, compounds bearing CA binding functional groups were tested for hCA I, II, IX and XII inhibition. The most active compounds were then assessed for their *in vitro* antiproliferative activities towards lung, liver and breast cancer cell lines followed by their toxicity towards normal human lung fibroblasts to evaluate their safety. As well, molecular docking studies were conducted to define binding interactions essential for biomolecular target recognition. Furthermore, *in silico* predictions of physicochemical and pharmacokinetic parameters were carried out to estimate their capacity as drug/lead-like candidates. Finally, representatives from the most active compounds were tested for their susceptibility to induce apoptosis and to modulate some underlying apoptotic markers.

### 2. Results and discussion

### 2.1. Chemistry

Dimroth triazole synthesis, or more specifically azide-enolate cycloaddition, was employed to obtain 1,4,5-trisubstituted 1,2,3-triazoles with variable chemical handles for derivatization [32]. The synthetic routes for the preparation of the intermediates and target compounds are outlined in Scheme 1. The key intermediates,

Fig. 1. Rationale for the design of the target compounds.

Scheme 1. Synthesis of the target 1,2,3-triazoles. Reagents and conditions: i)  $CH_3COCH_2COCH_3$ ,  $CH_3ONa$ ,  $CH_3ONa$ ,  $CH_3OH$ , stir overnight. ii)  $NH_2CONHNH_2$ .HCl,  $CH_3COONa$ ,  $C_2H_5OH$ , reflux for 8 h iii)  $NH_2CSNHNH_2$ , glacial  $CH_3COOH$ , reflux for 8–12 h, or fusion at 180 °C for 20 min. iv) 4- $CIC_6H_4COCH_2Br$ , few drops of  $(C_2H_5)_3N$  or pyridine,  $C_2H_5OH$ , reflux for 3–5 h. v)  $C_6H_3NHNH_2$ , few drops of  $CH_3COOH$ ,  $C_2H_3OH$ , reflux for 12–16 h. vi)  $C_3COOH$ ,  $C_3$ 

1-[1-(4-substituted phenyl)-5-methyl-1*H*-1,2,3-triazol-4-yl]ethanones (**2a-e**), were synthesized in good yields and with pure regioselectivity, via reacting aryl azides (**1a-e**) with acetylacetone in the presence of sodium methoxide/methanol. Condensation of the appropriate ketone (**2a-e**) with semicarbazide hydrochloride in the presence of sodium acetate in ethanol afforded the corresponding semicarbazones (**3a-e**). Whereas refluxing the ketones (**2a,c-e**) with thiosemicarbazide in glacial acetic acid or fusion of thiosemicarbazide with **2b** at 180 °C for 20 min yielded the corresponding thiosemicarbazones (**4a-e**). In addition, cyclization of

thiosemicarbazones (**4a-e**) with p-chlorophenacyl bromide in ethanol using catalytic amount of triethyl amine or pyridine furnished the corresponding thizaoles (**5a-e**). Hydrazones (**6a-e**) were synthesized by reacting the appropriate ketone (**2a-e**) with phenyl hydrazine in ethanol containing catalytic amount of acetic acid. Synthesis of the target pyrazole carbaldehydes (**7a-e**) was achieved by heating the appropriate phenylhydrazone derivative (**6a-e**) in a mixture of dimethylformamide and phosphorous oxychloride, following Vilsmeier Haack reaction conditions [33]. For compound **7e**, the *N*-thiazoly-2-yl sulfonamide was hydrolyzed to sulfonic acid

(see supporting information). Finally, the target aldoximes (**8a-d**) were attained by treating the respective carbaldehydes (**7a,b,d,e**) with a slight excess of hydroxylamine hydrochloride in the presence of sodium acetate/ethanol.

It is noteworthy to mention that compounds **4a-e**, **5a-e**, **6a-e** and **8a-d** exist solely as the favorable *E* geometric isomers as reported in literature for similar compounds [34–38]. Moreover, integrity of the structures of the newly synthesized compounds was substantiated by microanalytical analyses, IR, <sup>1</sup>H NMR, <sup>13</sup>C NMR and MS data (refer to chemistry experimental section and supporting information).

### 2.2. Biological evaluation

#### 2.2.1. In vitro COX-1 and COX-2 inhibitory activities

Compounds **2a-e**, **3a-e**, **4a-e**, **5a-e** and **8a-d** were tested for *in vitro* COX-1/COX-2 inhibitory activities using an ovine COX-1/human recombinant COX-2 assay kit (Catalog no. 560131; Cayman Chemicals Inc. Ann Arbor, MI, USA). Activities were expressed as concentrations producing 50% enzyme inhibition (IC $_{50}$   $_{\mu}$ M). Selectivity index (SI) values were also calculated as IC $_{50}$  (COX-1)/IC $_{50}$  (COX-2) to gauge their safety. The non-selective cyclooxygenase inhibitors (indomethacin and diclofenac) and the COX-2 selective inhibitor celecoxib were used as positive controls.

As outlined in Table 1; all compounds were more potent COX-2 inhibitors than indomethacin and diclofenac with two-digit nanomolar to submicromolar IC50 values (0.04–0.42  $\mu$ M). They displayed weak inhibition of COX-1 in comparison to indomethacin and diclofenac with IC50 values in the range of 5.6–14.2  $\mu$ M.

In comparison to celecoxib, compounds **5d**, **5e**, **8c** and **8d** were more potent as COX-2 inhibitors while compounds **4c-e**, **5b**, **8a** and **8b** were equipotent. In addition, compounds **4b**, **5a** and **5c** were nearly comparable to celecoxib.

Interestingly, all compounds displayed balanced weak COX-1 and more potent COX-2 inhibition with selectivity indices (SI) varying from 14 to 260. Compounds **5d**, **5e**, **8c** and **8d** had their SI values more than celecoxib (310–355 vs 294 for celecoxib, respectively). The aforementioned SI values are superior to non-selective COX inhibitors while those inferior to celecoxib, could also be regarded as advantageous by potentially avoiding the cardiovascular events associated with the highly selective COX-2 inhibitors [39].

A careful inspection of the structures of the tested compounds revealed that the starting triazolyl ethanones  $\bf 2a-e$  displayed submicromolar IC<sub>50</sub> values for COX-2 inhibition in the range of 0.11–0.42  $\mu$ M, albeit operating at one order of magnitude of activity higher than celecoxib. Among this series, the highest activity was observed with the chloro- and sulfonamide-substituted derivatives  $\bf 2a$  and  $\bf 2d$  while the carboxylic acid congener  $\bf 2c$  was the least active.

Condensation of **2a-e** into the semicarbazones **3a-e** did not improve COX-2 inhibitory activity (IC<sub>50</sub> = 0.27–0.42  $\mu$ M). They showed 12–19% the activity of celecoxib with their potencies in the following descending order: **3b** (F) > **3c** (COOH) > **3a** (Cl) > **3e** (sulfathiazole) > **3d** (SO<sub>2</sub>NH<sub>2</sub>).

Meanwhile, except for the chloro thiosemicarbazone **4a**, condensation of the ethanones **2b-e** into the thiosemicarbazones **4b-e** resulted in remarkable enhancement of COX-2 inhibitory activity expressed as two-digit nanomolar IC<sub>50</sub> values and higher selectivity indices (137.1–260). Replacement of the semicarbazone oxygen atom with a sulfur atom in compounds **4b-e** seemed to greatly influence the activity. This might be conferred to the larger size of the sulfur atom which is capable of occupying the wider cavity of COX-2 binding site along with the resultant molecular interactions. The carboxylic acid (**4c**), sulfonamido (**4d**) and

sulfathiazole (**4e**) derivatives **4e** were equipotent to the positive control celecoxib ( $IC_{50}=0.05~\mu M$ ). Whereas, the fluoro thiosemicarbazone **4b** exerted approximately 71% the activity of celecoxib.

Furthermore, cyclization of the thiosemicarbazones into the thiazole derivatives **5a-e** proved to be a favorable structural modification producing strong COX-2 inhibition with.

IC<sub>50</sub> values ranging from 0.04 to 0.07 μM. As observed with their precursors **4d** and **4e**, the sulfonamido **5d** and sulfathiazole **5e** derivatives were the most potent (IC<sub>50</sub> = 0.04 μM) in this series. They were even more potent (20% increase) and selective than celecoxib (SI = 310 and 355 Vs 294 for celecoxib). Other derivatives in this series displayed comparable potency to celecoxib (IC<sub>50</sub> = 0.05–0.07 μM) and were in the following order of activity; **5b** (F) > **5a** (CI) > **5c** (COOH).

Hybridization between triazole ring and pyrazole-4-carbaldehyde oxime fragment afforded compounds 8a-d, which were effective nanomolar inhibitors of COX-2 enzyme (IC $_{50}=0.04-0.05~\mu\text{M}$ ). Intriguingly, the sulfonamide 8c and the sulfonic acid derivative 8d achieved both 20% increase in activity and higher SI when compared to celecoxib. The sulfonamide derivative 8c demonstrated superior activity to celecoxib (IC $_{50}=0.042~\mu\text{M}$ ). The halogen-bearing derivatives 8a (Cl) and 8b (F) were equipotent to celecoxib.

Collectively, the thiosemicarbazones **4b-e**, thiazoles **5a-e** and pyrazoles **8a-d** exhibited potent nanomolar inhibition of COX-2 enzyme with IC<sub>50</sub> values ranging from 0.04 to 0.07  $\mu$ M.

### 2.2.2. In vitro 15-LOX inhibitory activity

The same twenty-four compounds were examined for their capability to inhibit 15-LOX enzyme in vitro using soybean 15-LOX inhibitor screening assay kit (Catalog no. 760700; Cayman Chemicals Inc. Ann Arbor, MI, USA). Both soybean and human 15-LOX enzymes share a high degree of structural homology reaching more than 50% around 10° A from the catalytic binding site [23]. The 12/15-LOX inhibitor, quercetin, was used as reference positive control [23]. Overall, all compounds operated at the same order of magnitude of activity as that of quercetin. More specifically, the thiosemicarbazones **4b-e**, thiazoles **5a-e** and pyrazole oximes **8ad** were significantly potent with  $IC_{50}$  values ranging from 1.19 (for **5e**) to 2.42 (for **4b**)  $\mu$ M, corresponding to approximately 2.8 and 1.4 times the activity of quercetin (IC<sub>50</sub> =  $3.34 \mu M$ ), respectively. Compounds  $\mathbf{2a}$  and  $\mathbf{2d}$  (IC<sub>50</sub> = 3.65  $\mu M$ ) were nearly as active as quercetin while the ethanones 2b, 2c and 2e, the semicarbazones **3a-e** and the thiosemicarbazone **4a** were less potent than quercetin (IC  $_{50} = 4.51 \text{--} 6.84~\mu\text{M}$  ). Intriguingly, 15-LOX inhibitory activities of the test compounds were concordant with their respective COX-2 inhibitory activities.

The following structure-activity correlations could be highlighted; cyclization of the thiosemicarbazone derived from the 4chlorophenyl azide 4a into the triazolyl thiazole 5a had a positive impact on activity shifting the IC<sub>50</sub> value from 5.33 to 1.68 μM. Along the same track, both the fluoro and sulfonamide thiazoles **5b,d** displayed higher activity than the precursor thiosemicarbazones 4b,d (1.83, 1.34 vs 2.42, 1.51, respectively). As for the sulfathiazole congener, its conversion from the thiosemicarbazone **4e** to the thiazole **5e** afforded the most potent 15-LOX inhibitor in the whole study (IC<sub>50</sub> = 1.19 vs 3.34  $\mu$ M for quercetin). The only exception for that trend was noticed with the carboxylic acid derivative where shifting from the thiosemicarbazone **4c** to the thiazole **5c** slightly reduced the activity. Regarding the triazolyl pyrazole oximes **8a-d**, the highest activity was achieved by the sulfonamido derivative **8c** showing IC<sub>50</sub> value of 1.29 µM making it the second most potent 15-LOX inhibitor in the study. Replacement of the -SO<sub>2</sub>NH<sub>2</sub> group in **8c** with -Cl group

 $\label{eq:compounds} \textbf{Table 1} \\ \textit{In vitro COX-1, COX-2, 15-LOX inhibitory IC}_{50} \ \text{values and COX SI values of the target compounds.}$ 

Cpd ID	Structure IC <sub>5</sub>			SI COX-1/COX-2 <sup>b</sup>	
		COX-1	COX-2	15-LOX	
Celecoxib	_	14.7	0.05	_	294.0
ndomethacin	_	0.04	0.49	_	0.08
Diclofenac Na	_	3.9	0.8	_	4.9
Quercetin	_ N	_ 7.9	_ 0.12	3.34 3.65	_ 65.8
2a	CI————————————————————————————————————	7.9	0.12	3.03	65.8
2b	$F \longrightarrow N \subset N$ $H_3C$ $CH_3$	7.3	0.23	4.75	31.7
2c	$HOOC \longrightarrow N \longrightarrow N \longrightarrow CH_3$	6.4	0.42	5.14	15.2
2d	$H_2NO_2S$ $N = N$ $N = N$ $CH_3$	7.6	0.11	3.65	69.1
2e	$S$ $HNO_2S$ $CH_3$ $H_3C$ $C$	5.8	0.29	4.72	20.0
<b>3</b> a	$CI \longrightarrow N = N $ $N = N $	5.6	0.32	6.84	17.5
3b	F—————————————————————————————————————	8.4	0.27	4.72	31.1
3c	$\begin{array}{c c} \text{HOOC} & & \\ \hline \\ \text{H_3C} & \\ \text{H_3C} & \\ \end{array} \begin{array}{c} \text{N} \\ \text{N} \\ \text{N} \\ \end{array} \begin{array}{c} \text{O} \\ \text{NH}_2 \\ \end{array}$	6.9	0.29	4.51	23.8
3d	$H_2NO_2S$ $N_2N$ $N_3C$ $N_3$	5.9	0.42	4.74	14.0
3e	$\begin{array}{c} \begin{array}{c} \begin{array}{c} \\ \\ \\ \end{array} \end{array} \\ \begin{array}{c} \\ \\ \end{array} \\ \begin{array}{c} \\ \\ \\ \end{array} \\ \begin{array}{c} \\ \\ \\ \end{array} \\ \begin{array}{c} \\ \\ \\ \end{array} \\ \\ \begin{array}{c} \\ \\ \\ \\ \\ \end{array} \\ \\ \begin{array}{c} \\ \\ \\ \\ \\ \end{array} \\ \\ \begin{array}{c} \\ \\ \\ \\ \\ \end{array} \\ \\ \begin{array}{c} \\ \\ \\ \\ \\ \end{array} \\ \\ \begin{array}{c} \\ \\ \\ \\ \\ \end{array} \\ \\ \begin{array}{c} \\ \\ \\ \\ \\ \end{array} \\ \\ \begin{array}{c} \\ \\ \\ \\ \\ \\ \end{array} \\ \\ \begin{array}{c} \\ \\ \\ \\ \\ \end{array} \\ \\ \begin{array}{c} \\ \\ \\ \\ \\ \end{array} \\ \\ \begin{array}{c} \\ \\ \\ \\ \\ \end{array} \\ \\ \begin{array}{c} \\ \\ \\ \\ \\ \end{array} \\ \\ \begin{array}{c} \\ \\ \\ \\ \\ \end{array} \\ \\ \begin{array}{c} \\ \\ \\ \\ \\ \\ \end{array} \\ \\ \begin{array}{c} \\ \\ \\ \\ \\ \\ \end{array} \\ \\ \begin{array}{c} \\ \\ \\ \\ \\ \\ \end{array} \\ \\ \begin{array}{c} \\ \\ \\ \\ \\ \\ \end{array} \\ \\ \begin{array}{c} \\ \\ \\ \\ \\ \\ \end{array} \\ \\ \begin{array}{c} \\ \\ \\ \\ \\ \\ \end{array} \\ \\ \begin{array}{c} \\ \\ \\ \\ \\ \\ \\ \end{array} \\ \\ \begin{array}{c} \\ \\ \\ \\ \\ \\ \\ \\ \end{array} \\ \\ \begin{array}{c} \\ \\ \\ \\ \\ \\ \\ \\ \end{array} \\ \\ \begin{array}{c} \\ \\ \\ \\ \\ \\ \\ \\ \end{array} \\ \\ \begin{array}{c} \\ \\ \\ \\ \\ \\ \\ \\ \end{array} \\ \\ \\ \\ \\ \\ \\ \\ \\ \\ $	7.9	0.34	6.52	23.2
<b>4</b> a	CI-N-N S N-N NH <sub>2</sub>	7.9	0.24	5.33	32.9
4b	$F \xrightarrow{N = N} N \xrightarrow{N = N} N \xrightarrow{N + 1} NH_2$	9.6	0.07	2.42	137.1
<b>4</b> c	N = N $N = N$ $N =$	11.6	0.05	1.65	232.0
4d	$H_2NO_2S$ $N = N$	13.0	0.05	1.51	260.0
<b>4</b> e	$\begin{array}{c} \begin{array}{c} \begin{array}{c} \\ \\ \\ \\ \end{array} \end{array} \begin{array}{c} \\ \\ \\ \\ \\ \\ \\ \\ \end{array} \begin{array}{c} \\ \\ \\ \\ \\ \end{array} \begin{array}{c} \\ \\ \\ \\ \\ \\ \end{array} \begin{array}{c} \\ \\ \\ \\ \\ \end{array} \begin{array}{c} \\ \\ \\ \\ \\ \\ \\ \end{array} \begin{array}{c} \\ \\ \\ \\ \\ \\ \\ \end{array} \begin{array}{c} \\ \\ \\ \\ \\ \\ \\ \end{array} \begin{array}{c} \\ \\ \\ \\ \\ \\ \\ \end{array} \begin{array}{c} \\ \\ \\ \\ \\ \\ \\ \end{array} \begin{array}{c} \\ \\ \\ \\ \\ \\ \\ \end{array} \begin{array}{c} \\ \\ \\ \\ \\ \\ \\ \\ \end{array} \begin{array}{c} \\ \\ \\ \\ \\ \\ \\ \\ \end{array} \begin{array}{c} \\ \\ \\ \\ \\ \\ \\ \\ \end{array} \begin{array}{c} \\ \\ \\ \\ \\ \\ \\ \\ \\ \\ \end{array} \begin{array}{c} \\ \\ \\ \\ \\ \\ \\ \\ \\ \\ \\ \\ \\ \end{array} \begin{array}{c} \\ \\ \\ \\ \\ \\ \\ \\ \\ \\ \\ \\ \\ \\ \\ \\ \\ \\ \\$	10.3	0.05	1.69	206.0
5a	CI—N=N S—CI	11.9	0.06	1.68	198.3

(continued on next page)

Table 1 (continued)

Cpd ID	Structure	$IC_{50} \mu M^a$			SI COX-1/COX-2 <sup>b</sup>
		COX-1	COX-2	15-LOX	
5b	F-N=N S CI	11.9	0.05	1.83	238.0
5c	HOOC - N=N S N N N N N N N N N N N N N N N N N	10.9	0.07	1.76	155.7
5d	$H_2NO_2S$ $N_2N$ $N_3$ $N_4$ $N_4$ $N_5$	12.4	0.04	1.34	310.0
5e		14.2	0.04	1.19	355.0
8a	CI CH <sub>3</sub> N-N	12.9	0.05	1.47	258.0
8b	N=N CH <sub>3</sub> N-N	10.9	0.05	1.98	218.0
8c	H <sub>2</sub> NO <sub>2</sub> S CH <sub>3</sub> N-N	12.4	0.04	1.29	310.0
8d	HO <sub>3</sub> S CH <sub>3</sub> N-N	13.9	0.04	1.91	347.5

<sup>&</sup>lt;sup>a</sup> IC<sub>50</sub> is the concentration (μM) required to produce 50% inhibition of COX-1, COX-2 and 15-LOX enzymatic activity. All values are expressed as mean of three replicates with standard deviation less than 10% of the mean.

in **8a** slightly decreased the activity, which was further reduced upon substitution with -F (**8b**) and -SO<sub>3</sub>H groups (**8d**).

Exhaustively, 15-LOX inhibition assay results proposed compounds **4c-e**, **5a-e** and **8a-d** as good single-digit micromolar inhibitors with IC<sub>50</sub> values in the range of 1.19–1.98  $\mu$ M.

Cognizant of our aim to target human LOX, we acknowledge the necessity of validating the activity of these compounds against the human enzyme. As well, it is equally important to confirm LOX inhibition via gauging its downstream products in cell-based assays. Indeed, our selection of targeting 15-LOX enzyme in the present study was based on the fact that our group previously proved the ability of some 1,2,3-triazoles to reduce 20-HETE production in THP-1 monocytes [23].

### 2.2.3. Carbonic anhydrase inhibition

The most active compounds in COX/LOX inhibition assays as well as those carrying CA-binding functionalities were tested *in vitro* for their inhibitory activity against the physiologically relevant hCA isoforms I, II, IX and XII by means of the stopped-flow carbon dioxide hydration assay [40]. Their activities were compared to the standard CA inhibitor acetazolamide (AAZ).

On the basis of the kinetic data reported in Table 2, triazole

derivatives 2d-e, 3d-e, 4b-e, 5a,c-e and 8a-d showed remarkable variation among the different CA isoforms and the following structure—activity-relationships (SARs) can be drawn:

- i) As far as the activity against the cytosolic widespread enzyme hCA I was concerned, it was efficiently inhibited by compounds carrying primary sulfonamide moiety (2d, 3d, 4d and 5d) in the medium nanomolar range (K<sub>i</sub> 73.0–252.0 nM), with the exception of compound 8c (Ki 4626 nM). On the other hand, introduction of secondary sulfonamide group on compounds 2e, 3e, 4e and 5e led to either a drastic decrease in their potency, showing high micromolar range (Ki 46,328-51001 nM) or a complete loss of activity as seen with derivatives 4e and 5e. An interesting inhibition profile was observed for compound 5c in which it was capable of inhibiting this isoform in the medium nanomolar range (Ki 550.8 nM) as well as hCA II (Ki 565.7 nM), without bearing the well-known sulfonamide zinc binding group. Moreover, the sulfonic acid derivative (8d) showed a weak inhibition against hCA I (Ki 18,340 nM).
- ii) The second abundant human cytosolic isoform, hCA II, was strongly inhibited by derivatives carrying primary

 $<sup>^{</sup>b}$  Selectivity index (SI) = IC<sub>50</sub> (COX-1)/IC<sub>50</sub> (COX-2).

**Table 2**Inhibition data of human CA isoforms hCA I, II, IX and XII for 2d-e, 3d-e, 4b-e, 5a,c-e and 8a-d derivatives using the standard acetazolamide (AAZ) by a stopped flow CO<sub>2</sub> hydrase assay.

Cpd ID	$K_i^* (nM)^a$			
	hCA I	hCAII	hCA IX	hCA XII
2d	73.0	7.9	9118	82.6
2e	51,001	6280	>100,000	>100,000
3d	212.6	16.4	4218	19.8
3e	46,328	6864	>100,000	>100,000
4b	>100,000	>100,000	>100,000	>100,000
4c	>100,000	416.1	>100,000	>100,000
4d	83.5	31.9	7270	15.3
<b>4e</b>	>100,000	62,533	>100,000	>100,000
5a	>100,000	>100,000	>100,000	>100,000
5c	550.8	565.7	>100,000	>100,000
5d	252.0	14.1	7893	13.4
5e	>100,000	>100,000	>100,000	>100,000
8a	>100,000	>100,000	>100,000	>100,000
8b	>100,000	>100,000	>100,000	>100,000
8c	4626	239.2	2254	154.4
8d	18,340	7710	>100,000	>100,000
AAZ	250	12.1	25.8	5.7

<sup>\*</sup> The inhibition constant, K<sub>i</sub>, denotes the equilibrium constant of the dissociation of the inhibitor-bound enzyme complex.

sulfonamide moiety (2d, 3d, 4d and 5d) in low nanomolar range ( $K_i$  7.9–31.9 nM) and, as mentioned above, when primary sulfonamide is replaced by a secondary one, the potency drastically decreased to the micromolar range ( $K_i$  6280–62533 nM). The medium nanomolar activities of derivatives 4c and 5c ( $K_i$  416.1–565.7 nM) might be attributed to the good zinc binding capability of carboxylic group. Interestingly, compound 4c showed selective inhibition against this isoform. Again, sulfonic acid 8d showed a weak inhibition against hCA II ( $K_i$  7710 nM).

- iii) The membrane-bound, tumor-associated, hCA IX, was weakly inhibited by primary sulfonamide compounds 2d, 3d, 4d and 5d (K<sub>i</sub> 2254–9118 nM) and the remaining compounds, here reported, did not show any significant inhibition against this isoform.
- iv) The second membrane-bound, tumor-associated, hCA XII, was efficiently inhibited by compounds with primary sulfonamide moiety (2d, 3d, 4d and 5d) in the low nanomolar range (K<sub>i</sub> 13.4–82.6 nM) and derivative 8c in medium nanomolar range with K<sub>i</sub> 154.4 nM. On the other hand, compounds bearing a secondary sulfonamide or other zinc binding groups did not show any significant inhibition against hCA XII.

### 2.2.4. In vitro anti-proliferative activity

The most active compounds in the aforementioned *in vitro* enzymatic assays were evaluated for their cytotoxic effects against normal human lung fibroblasts (WI-38) using 5-fluorouracil (5-FU) as reference applying sulforhodamine B (SRB) assay protocol [41,42]. As shown in Table 3, IC<sub>50</sub> values recorded for the test compounds were in the range of 364.9–479.6  $\mu$ M, compared to 78.5  $\mu$ M for 5-FU, and hence, indicating their safety. In comparison to celecoxib (IC<sub>50</sub> = 432.9  $\mu$ M), compounds **4c**, **4e**, **5c**, **5e** and **8d** exhibited higher safety margin (IC<sub>50</sub> = 449.5–479.6  $\mu$ M).

Anti-proliferative activity of compounds **2d**, **3d**, **4b-e**, **5a-e** and **8a-d** was evaluated against three cancer cell lines namely; non-small cell lung cancer A549, liver cancer HepG2 and breast cancer MCF-7 cell lines. Celecoxib and 5-FU were used as reference drugs.

**Table 3** Cytotoxicity ( $IC_{50}$ ,  $\mu M$ ) of selected compounds towards human lung fibroblast non-tumoral cell line (WI-38) and their percentage inhibition (at 100  $\mu M$ ) of lung A549, liver HepG2 and breast MCF7 cancer cell lines.

Cpd ID	$IC_{50} (\mu M)^a$	% Inhibitio	n <sup>a</sup> (100 μM)	
	WI-38	A549	HepG2	MCF7
2d	390.6	NIb	3.61	17.68
3d	364.9	18.17	NI	5.80
4b	405.8	NI	19.76	6.52
4c	479.6	NI	NI	46.64
4d	377.5	3.88	NI	36.12
4e	458.3	11.33	22.12	20.71
5a	378.9	77.53	74.4	91.30
5b	413.7	11.95	20.73	33.46
5c	460.7	67.00	1.41	40.44
5d	388.4	68.10	59.05	37.20
5e	467.7	51.14	56.01	39.94
8a	402.5	69.73	78.98	97.85
8b	393.4	92.42	88.99	98.21
8c	378.9	12.29	7.68	83.44
8d	449.5	NI	12.47	43.54
Celecoxib	432.9	86.15	77.88	89.86
5-FU	78.5	89.29	80.67	90.72

<sup>&</sup>lt;sup>a</sup> All values are expressed as mean of three replicates with standard deviation less than 10% of the mean.

Results are listed in Table 3, and expressed as percentage inhibition values at a concentration of 100  $\mu$ M.

Generally speaking, anticancer activity was more pronounced among the triazolyl thiazoles (**5a,c-e**) and triazolyl pyrazoles (**8a-c**). Regarding activity against A549 cell line, compound 8b showed the highest % inhibition (92.42%) compared to 86.15 and 89.29% for celecoxib and 5-FU, respectively. Compounds 5a,c-e and 8a displayed percentage growth inhibition in the range of 51.14–77.53%. As for HepG2 cell line, almost the same pattern of activity was observed with 89% inhibition shown by compound 8b. While compounds **5a,d,e** and **8a** exhibited 56.01–78.98% inhibition, compared to 77.88 and 80.67% for celecoxib and 5-FU, respectively. As far as MCF7 cell line was concerned, it was the most susceptible cell line, with compounds 5a and 8a,b showing higher magnitude of activity (91.30-98.21% inhibition) with respect to both reference drugs (89.86 and 90.72% for celecoxib and 5-FU, respectively) and other cell lines as well. As an exception, compound 8c exerted lower percentage inhibition (83.44%) than the reference drugs.

The most potent seven compounds showing more than 50% inhibition on the respective sensitive cell lines were further tested for IC<sub>50</sub> values calculations as illustrated in Table 4. Compounds **5a** and **8b,c** showed significant growth inhibitory activity with single-digit micromolar IC<sub>50</sub> values in the range of 2.37–8.9  $\mu$ M. In detail,

**Table 4** *In vitro* anti-proliferative activity of the most active compounds 5a,c-e and 8a-c against lung A549, liver HepG2 and breast MCF7 cancer cell lines.

Cpd ID	$IC_{50} (\mu M)^a$				
	A549	HepG2	MCF7		
	8.9	2.37	2.69		
5c	73.1	_	_		
5d	28.5	72.4	_		
5e	99.3	89.5	_		
8a	55.7	26.5	21.97		
8b	27	31.1	5.32		
8c	_	_	3.2		
Celecoxib	17.5	0.36	2.56		
5-FU	0.69	0.52	0.59		

<sup>&</sup>lt;sup>a</sup> All values are expressed as mean of three replicates with standard deviation less than 10% of the mean.

<sup>&</sup>lt;sup>a</sup> Mean from 3 different assays, by a stopped flow technique (errors were in the range of  $\pm$  5–10% of the reported values).

b NI = no inhibition.

IC<sub>50</sub> values for compound **5a** were 8.9, 2.37 and 2.69 μM against A549, HepG2 and MCF7 cell lines, respectively. It was two times as potent as celecoxib (17.5  $\mu M$ ) on A549 and almost equipotent on MCF7 (2.56  $\mu$ M) cell line. Other triazolyl thiazoles **5c-e** displayed weak activities with IC50 values in the range of 72.4–99.3  $\mu M$ except for compound 5d which exhibited moderate activity on A549 cell line (28.5 μM). With regard to the triazolyl pyrazole oximes series, compound 8a exerted moderate activity against both HepG2 and MCF7 cell lines (26.5 and 21.97 μM, respectively) while its activity against A549 cell line was weak (55.7  $\mu$ M). Whereas compound 8b demonstrated moderate activity against A549 and HepG2 cell lines (27 and 31.1 µM, respectively). Additionally, it showed almost one half the potency of celecoxib on MCF7 cell line (5.32 and 2.56  $\mu$ M, respectively). Along the same line, compound **8c** showed 80% the activity of celecoxib on MCF7 cell line. Generally, all compounds were less potent than the standard 5-FU on the three tested cell lines.

### 2.2.5. Inhibition of 6-keto-prostaglandin-F1 $\alpha$ expression cell-based assay

To further confirm the inhibitory activity of **5a** and **5d** on COX-2 enzyme, the effect of these compounds on the production of 6keto-PGF1α was evaluated. 6-Keto-PGF1α is a prostacyclin metabolite commonly used in the literature to reflect endogenous COX-2 activity [43,44]. For this purpose, two COX-2 expressing cancer cell lines, HT-29 and THP-1 macrophages, were used [45,46]. Prior to 6keto-PGF1α ELISA, a cytotoxicity assay of the compounds was conducted for each cell line. Compounds 5a, 5d, and the reference diclofenac demonstrated a concentration-dependent cytotoxicity (Fig. 2A). Thus, drug concentrations yielding equal cell viability were selected for the ELISA assay for relevant comparison. In line with the differences in the measured IC<sub>50</sub> values of COX-2 inhibition between diclofenac, **5a**, and **5d** (0.8, 0.06, and 0.04  $\mu$ M, respectively), treatment of cells by 5a and 5d led to a great reduction in 6-keto-PGF1 $\alpha$  concentration compared to diclofenac. LPS-challenged HT-29 cells treated with **5a** and **5d** produced much less 6-keto-PGF1 $\alpha$  (C<sub>5a</sub> = 2.1 pg/ml and C<sub>5d</sub> = 3.2 pg/ml) in comparison to the COX inhibitor diclofenac ( $C_{diclo}=26.98\ pg/ml$ ). A similar observation was seen with THP-1 cells ( $C_{5a}=3.31\ pg/ml$ ,  $C_{5d} = 8.15 \text{ pg/ml}$ , and  $C_{diclo} = 21.65 \text{ pg/ml}$ ). Altogether, these results confirm the inhibitory actions of these drugs on the production of COX-2 metabolites, hence COX-2 enzyme activity.

Of peculiar interest in this experiment is the difference in cytotoxic effect between the two cell lines despite equal inhibition of the COX-2 product metabolite by **5a** and **5d** (Fig. 2A). Particularly, **5d** did not lead to any appreciable cell death in THP-1 cells despite that both **5a** and **5d** showed potent cytotoxicity on HT-29 cell. This might be attributed to the CA inhibitory effect exerted by **5d**, since HT-29 cells are known to have a much higher basal expression of CA than THP-1 cells [47].

### 2.2.6. Investigation of apoptotic capacity of compounds **5a** and **5d** in MCF-7 cells

Apoptosis is a type of programmed cell death. Its dysregulation is commonly connected to diseased states such as cancer [48]. It is mediated through the activation of a proteolytic caspase cascade, which can be grouped into initiator and effector caspases. Initiator caspases (2, 8, 9, and 10) launch the process and effector caspases (3, 6, and 7) break down molecules that are vital for cell survival [48].

This quality control machinery is also regulated by the Bcl family of proteins which comprise proapoptotic and antiapoptotic proteins. Bcl-2 associated X protein (Bax) and Bcl-2 antagonist killer (Bak) belong to the proapoptotic members [48]. While, Bcl-2 and Bcl-xL possess antiapoptotic functions. The balance between proand antiapoptotic proteins dictates the fate of a cell [48].

On the other hand, the correlation between the arachidonate pathway enzymes (COX-2 and LOX) and downregulation of apoptosis, has been recently established [6,15]. In addition, prior studies pointed out the role of carbonic anhydrase XII inhibition in induction of apoptosis in T-cell lymphomas [49]. Hence, we investigated the apoptosis-inducing capability of two of the most active compounds (**5a** and **5d**) via cell cycle analysis and determination of levels of expression of some representative apoptotic markers.

2.2.6.1. Flow cytometric cell cycle analysis. Targeting phases of the cell cycle of cancerous cells has been largely pursued for anticancer outcomes. Hence, the effect of the most active compounds **5a** and **5d** on cell cycle distribution in MCF-7 and A549 cells, respectively, was analyzed (Fig. 3). Results of the DNA flow cytometric assay

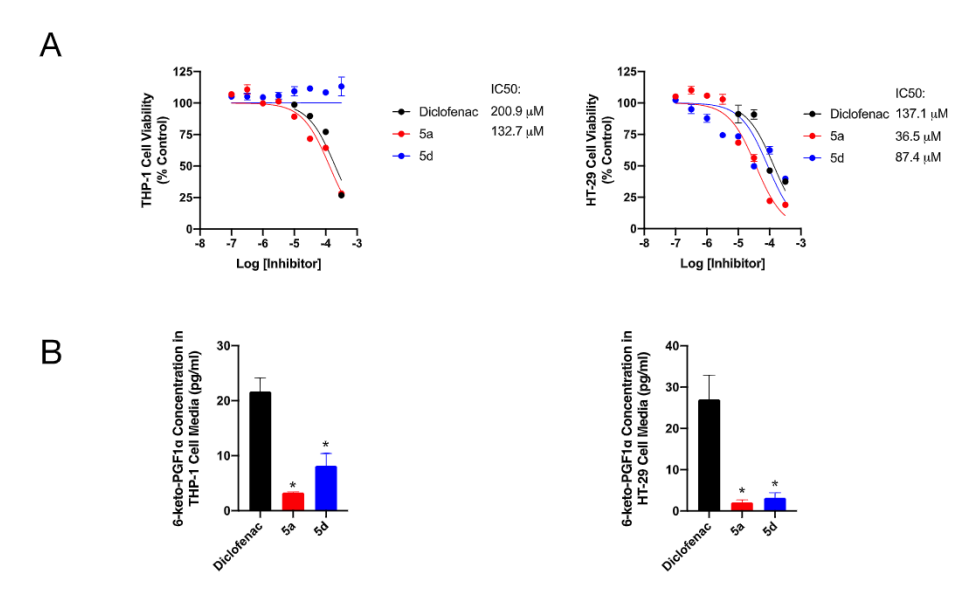


Fig. 2. A, Cytotoxicity of diclofenac, 5a, and 5d on THP-1 cells (human acute monocytic leukaemia) and HT-29 cells (human colorectal adenocarcinoma). B, Inhibition of 6-keto-PGF1 $\alpha$  production in THP-1 and HT-29 cells by 100 μM of 5a and 5d compared to diclofenac (300 μM, a concentration yielding equal cytotoxicity). \* denotes a *P*-value < 0.05 vs. diclofenac assessed by one-way ANOVA followed by Tukey multiple comparisons test.

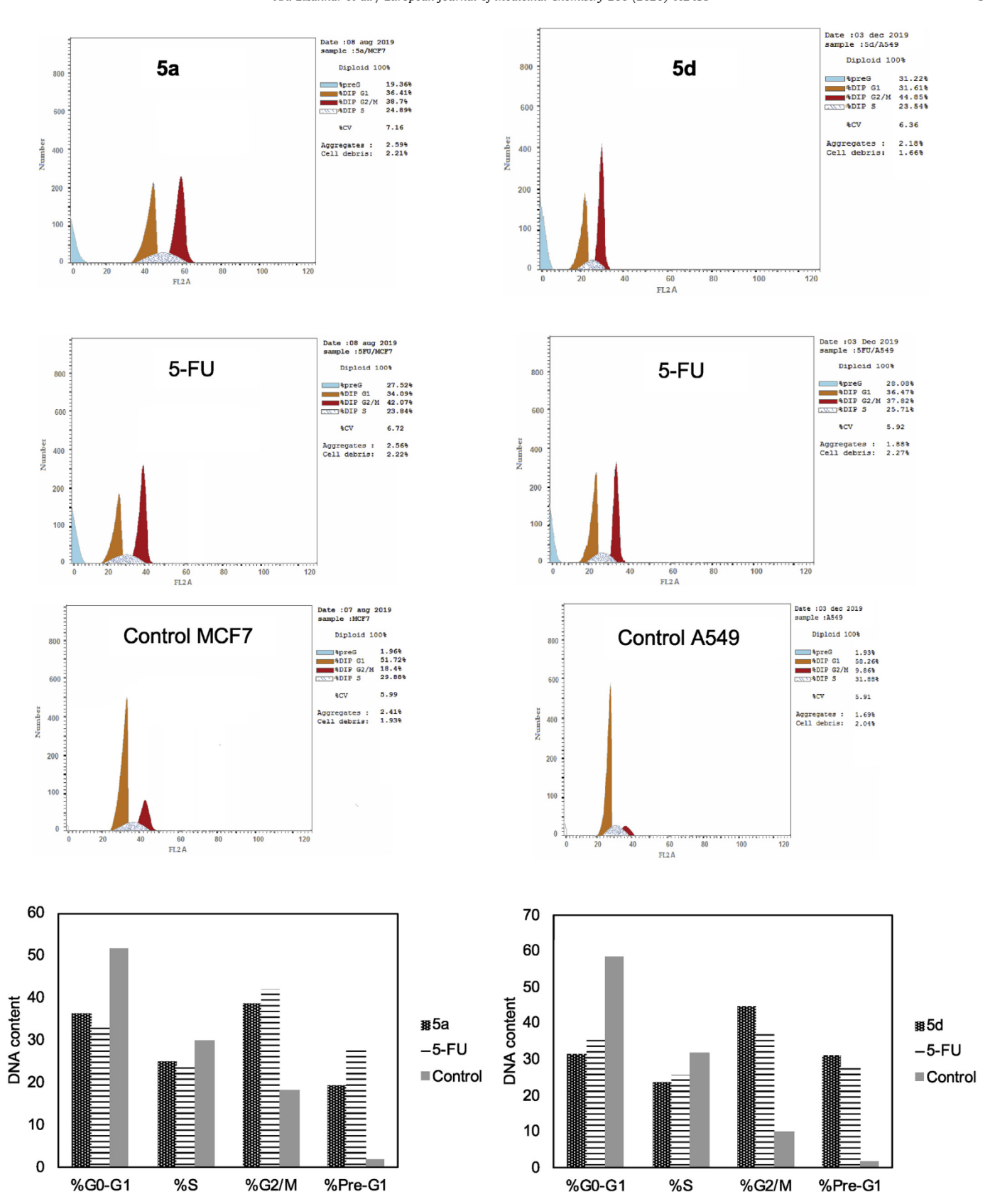


Fig. 3. Effect of compounds 5a (left panel) and 5d (right panel) on the phases of cell cycle in comparison to 5-FU and control in MCF7 and A549 cells, respectively.

showed that the percentage of MCF-7 cells in G0/G1 phase of the cell cycle was reduced from 51.72% in the control to 36.41% and 34.09% (corresponding to 1.4- and 1.5-folds decrease compared to control) after treatment with compound **5a** and 5-FU, respectively. As for the S phase, the percentage of cells slightly decreased from 29.88% to 24.89% and 23.84% for the untreated, 5a-treated and 5-FU-treated cells, respectively. This was accompanied by a notable rise in percentage of MCF-7 cells at the G2/M phase from 18.4% to 38.7% and 42.07% (corresponding to 2.1- and 2.3-folds increase compared to control) for the control, 5a-treated and 5-FU-treated cells, respectively. Besides, Pre-G1 phase recorded an increase in DNA content from 1.96% to 19.36% and 27.52% (corresponding to 9.9- and 14-folds increase compared to control) for the untreated, **5a**-treated and 5-FU-treated cells, respectively. Along the same line, compound **5d** affected cell cycle phases of A549 cells in a similar fashion to **5a** on MCF7. Of particular interest, G2/M phase demonstrated an increase in DNA content from 9.86% to 44.85%, corresponding to 4.5-folds increase with respect to control while 5-FU led to only 37.82%. Intriguingly, DNA content observed in Pre-G1 phase was 31.22% (for 5d) and 28.08% (for 5-FU) from 1.93% for control cells.

Based on the aforementioned data, increased DNA content at Pre-G1 and G2/M phases clearly suggested that apoptosis induction and G2/M cell growth arrest to be partially responsible for the anticancer effect of compounds **5a** and **5d**.

2.2.6.2. Annexin V-FITC/propidium iodide analysis of apoptosis. To further confirm the apoptotic-inducing potential of compounds **5a** and **5d** in MCF-7 and A549 cells, respectively, dual staining assay with annexin V-FITC/propidium iodide (AV/PI) was conducted (Fig. 4 and Table 5).

This analysis revealed that treatment of MCF-7 cells with

compound **5a** afforded a considerable increase in the percentage of annexin V-FITC-positive apoptotic cells, comprising both the early (from 0.4% to 5.88% and 7.26% for compound **5a** and 5-FU, respectively) and late apoptotic (from 0.29% to 11.29% and 17.71% for compound **5a** and 5-FU, respectively) phases. Hence, compound **5a** displayed about 25-folds total apoptotic increase, when compared to control along with showing 70% the apoptotic capacity of 5-FU. In A549 cells, the percentage of annexin V-FITC-positive early apoptotic cells increased from 0.63% to 9.15% and 4.29% upon treatment with **5d** and 5-FU, respectively. While, late apoptotic cells changed from 0.29% to 19.56% (for **5d**) and 20.68% (for 5-FU). Therefore, compound **5d** produced an overall apoptotic increase of 31- and 1.2-folds in comparison to control and 5-FU, respectively.

2.2.6.3. Effect on the expression levels of the initiator caspase-9 and mitochondrial apoptotic markers Bcl-2 and bax. Being one of the components of the intrinsic signaling pathway activating apoptosis [48], the expression level of the initiator caspase-9 was probed upon treatment of MCF-7 and A549 cells with compounds **5a** and **5d**, respectively, and compared to 5-FU. Data presented in Table 6 showed that compounds **5a** and **5d** produced 7.36- and 10.56-folds increase in the expression level of caspase-9 in comparison to controls. This represented 62% and 91% of the increase caused by 5-FU.

In order to gain more clues about the mechanisms by which these compounds can induce apoptosis, we examined their impact on the proapoptotic Bax and antiapoptotic Bcl-2 proteins. Results demonstrated that compounds **5a** and **5d** upregulated the expression of Bax by 5- and 7.82-folds in comparison to control, representing around 78% and 88% of the increase brought about by 5-FU, respectively. Furthermore, Bcl-2 expression level was downregulated upon treatment with compound **5a**, from 7.49 to 4.02 and

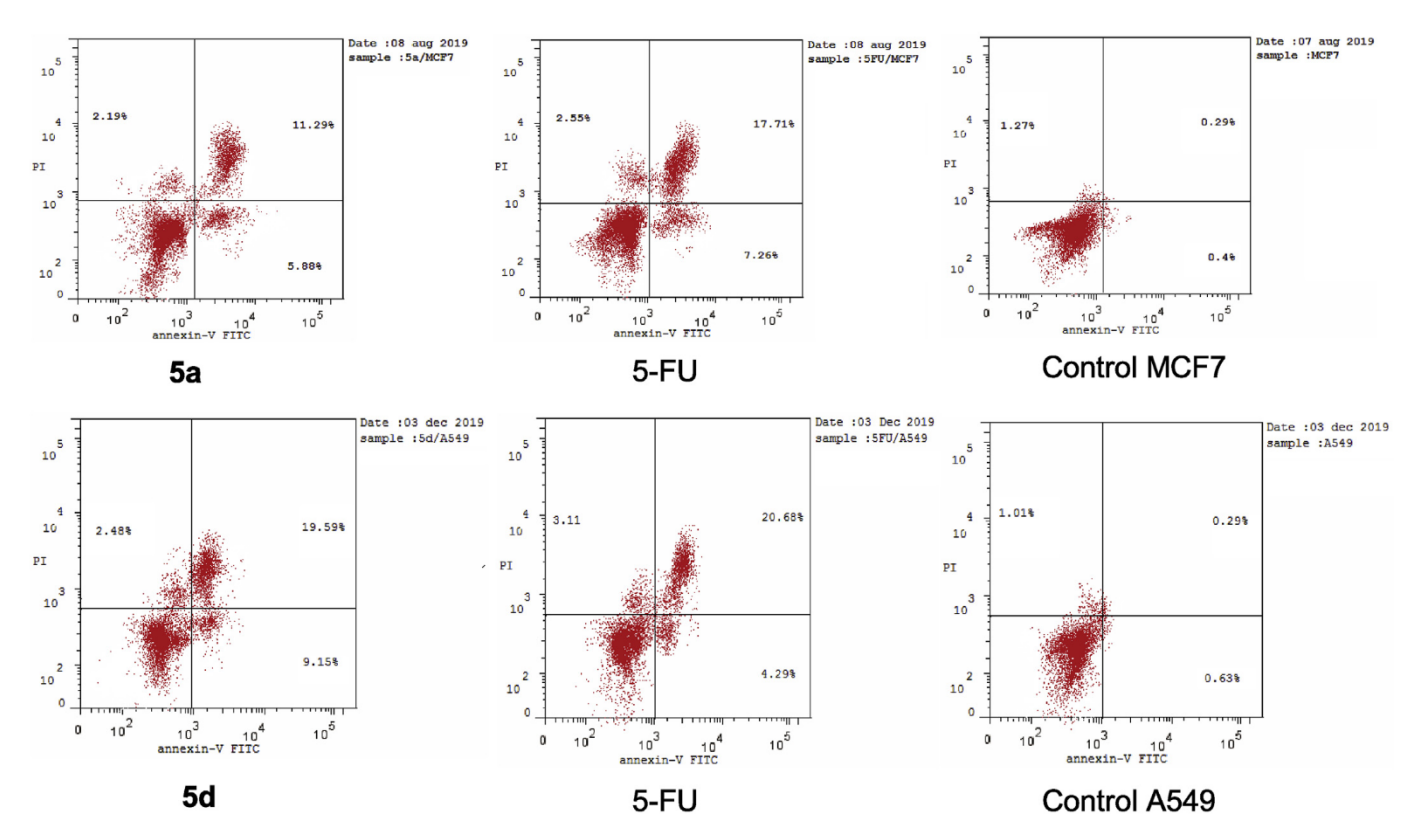


Fig. 4. Effect of compounds 5a (upper panel) and 5d (lower panel) on the percentage of annexin V-FITC-positive staining in MCF-7 and A549 cells, respectively. Experiments were performed in triplicates. The four quadrants identified as: LL: viable; LR: early apoptotic; UL: necrotic.

**Table 5**Distribution of apoptotic cells in the annexin V-FITC experiment.

Cell line	Cpd ID	Apoptosis		Necrosis	
		Early (Lower Right %)	Late (Upper Right %)	Total	
	5a	5.88	11.29	17.17	2.19
MCF7	5-FU	7.26	17.71	24.97	2.55
	Control	0.4	0.29	0.69	1.27
	5d	9.15	19.59	28.74	2.48
A549	5-FU	4.29	20.68	24.97	3.11
	Control	0.63	0.29	0.92	1.01

**Table 6**Effect of compounds 5a and 5d on the expression levels of active caspase-9, Bax and Bcl-2 in MCF-7 and A549 cancer cells, respectively.

Cell line	Cpd ID	Caspase-9		Bax	Bax		Bcl-2	
		Conc. (ng/ml)	Fold change	Conc. (pg/ml)	Fold change	Conc. (ng/ml)	Fold change	
MCF7	5a	13.02 ± 0.8	7.36	227.2 ± 13.4	4.99	4.02 ± 0.2	0.54	
	5-FU	$20.87 \pm 1.5$	11.80	$289.9 \pm 8.6$	6.37	$2.23 \pm 0.2$	0.3	
	Control	$1.77 \pm 0.1$	1	$45.46 \pm 3.6$	1	$7.49 \pm 0.1$	1	
A549	5d	$12.69 \pm 0.3$	10.56	$329.7 \pm 6.3$	7.82	$4.59 \pm 0.2$	0.51	
	5-FU	$13.98 \pm 0.2$	11.63	$376.9 \pm 8.2$	8.93	$6.21 \pm 0.2$	0.68	
	Control	$1.2 \pm 0.1$	1	$42.16 \pm 6.2$	1	$9.04 \pm 0.1$	1	

2.23 ng/ml for the control, compound **5a** and 5-FU, respectively. Whereas compound **5d** afforded more reduction in Bcl-2 expression than 5-FU (from 9.04 (control) to 4.59 and 6.21 ng/ml, respectively) (Table 6).

### 2.2.7. In vivo antitumor activity in MCF-7 xenograft model

Given the significant CA XII and COX-2/15-LOX inhibitory activities and *in vitro* anti-proliferative effect of compound **8c** (as a representative of the most active compounds), MCF-7 xenograft model in immunocompromised BALB/c mice was established to assess if the *in vitro* activity could be mirrored *in vivo*. First, LD<sub>50</sub> values were determined in newborn BALB/c mice [50] and found to be 61.67 mg/kg for compound **8c** and 57.2 mg/kg for 5-FU.

For immunosuppression, the mice received cyclosporin A (CsA, Abcam) [51]. About 1 million MCF-7 cells in 100  $\mu$ l of DMEM were injected subcutaneously in abdominal fats of each animal (26–38 g) to establish the xenograft model [52]. When the tumor volume reached around 1 cm³, the tumor-bearing mice were randomly divided into three groups; the control (vehicle-treated) group, compound **8c**-treated group and 5-FU treated group. An intraperitoneal injection [14] of 23 mg/kg thrice a week, for each of **8c** and 5-FU for 28 days was given. Tumor volume and mice body weights were recorded every 7 days and the whole treatment period lasted for four weeks.

As shown in Fig. 5, there was a rapid increase in tumor volume for the control group, while both **8c** and 5-FU treated groups

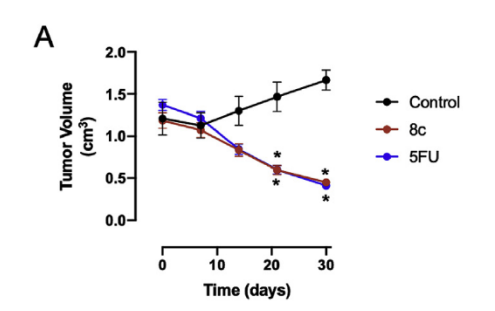
showed decrease in tumor volume. Similar patterns for tumor volume reduction were observed for both drugs along the treatment period. After 28 days, the final tumor volumes for these two groups were 0.45 and 0.41 cm<sup>3</sup>, respectively. Furthermore, only slight decrease was observed in the body weight of **8c**-treated group (from 29.8 g at day 0–27.3 g at day 28) indicating low-grade toxicity when compared to the control group (from 31.3 g at day 0–22.9 g at day 28). Whereas the decrease in body weight for the 5-FU treated group was from 31.3 g at day 0–24.5 g at day 28. Hence, compound **8c** demonstrated promising potential for the development of CA XII, COX-2/15-LOX multi-target inhibitors for cancer therapy.

### 2.3. Molecular modeling

In order to explain the possible binding modes and molecular interactions behind the inhibitory activities of the most active compounds (**5a**, **5d**, **8b** and **8c**), molecular docking studies were conducted using Molecular operating environment software (MOE, 2016.0802).

Choice of the docking poses relied on the top-scored conformations along with favorable binding interactions. Binding affinities to the studied enzymes were estimated based on docking scores, hydrogen bonds, and the relative positioning of the docked compounds with respect to the co-crystallized ligands.

Molecular docking protocol was validated by re-docking the co-



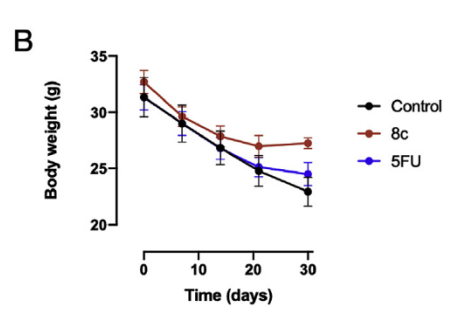


Fig. 5. In vivo antitumor effect of 8c and 5-FU on MCF-7 xenograft model. Tumor volumes (A) and body weights (B) were recorded on days 0, 7, 14, 21 and 28 after ip administration of 8c and 5-FU at a dose of 23 mg/kg thrice a week. \* denotes a P-value < 0.05 vs. control assessed by two-way ANOVA followed by Sidak multiple comparisons test.

crystallized ligands; S58 (for COX-2), RS7 (for 15-LOX), A6N (for CA II) and AZM (for CA XII) into the respective enzyme binding sites (refer to Figures **SM1-SM4**, supporting information for interactions of crystal structures). The original poses generated from PDB were retrieved with root mean square deviation (RMSD) values in the range of 0.218–1.6 Å and binding energy scores of -7.17 to -9.31 kcal/mol. This proved the robustness and reliability of the used docking protocols.

The postulated docked poses for compounds 5a and 5d (Figs. 6 and 7) in their E-configuration, into COX-2 enzyme (PDB code 1CX2), showed that they occupied COX-2 active site and were stabilized by a number of hydrophobic and polar interactions. The p-chloro or sulfonamidophenyl ring lied deeply into the hydrophobic pocket formed by amino acid residues Arg120, Leu359 and Leu531. Further stabilization of **5a** occurred via pi-cation interaction between p-chlorophenyl ring and Arg120 while for 5d a hydrogen bond was formed between one of the sulfonamide oxygens and Arg120 as well. Other interactions like pi-hydrogen bonds were observed between thiazole ring of 5a and the key amino acids Val523 and Ser353 along with hydrogen bond between imine nitrogen and Ser353. As for 5d, hydrogen bonds were noticed between sulfonamide oxygen and Tyr355, thiazole ring nitrogen and Gly354 and hydrazineyl NH and Gln192. In addition, pi-hydrogen contacts were formed between p-sulfonamidophenyl ring and Tyr355 and triazole ring and Ser353.

With regard to the binding modes of compounds **8b** and **8c** (Figs. 8 and 9), they perfectly lodged into the inner hydrophobic cleft of the active site formed by amino acid residues Arg120, Leu359 and Leu531. Binding was strengthened by formation of pication interaction between phenyl ring and the essential amino acid residue Arg120. Also, pi-hydrogen bond was detected between phenyl ring and Tyr355 and hydrogen bond between triazole ring nitrogen and Phe518. For compound **8c**, extra hydrogen bond interaction was found between p-sulfonamidophenyl ring and Leu352.

Analysis of the most energetically profitable poses of compounds **5a**, **5d**, **8b** and **8c** into 15-LOX enzyme (PDB code 1LOX) showed that they accommodated perfectly into the hydrophobic U-shaped cavity of the enzyme active site, where the catalytic iron sit near to its base, in coordination with histidines 361, 366, 545 and Ile663.

The four compounds were surrounded by side chains of hydrophobic amino acids Phe175, Phe353, Leu362, Phe415, Met419, Ile593 and Leu597. For compounds 5a and 5d (Figs. 10 and 11), they showed exactly the same binding pattern where hydrogen bond was formed between Ala404 and triazole ring nitrogen. Also, four pi-hydrogen bonds were formed between thiazole ring and Glu357,

the pharmacophoric thiazole and triazole rings and Leu 408 and finally between p-chloro or sulfonamidophenyl rings and Phe175. An extra hydrogen bond was noticed between one of the sulfonamide oxygens of 5d and Gln596.

Upon docking the pyrazole oxime **8b** (Fig. 12), pi-hydrogen interaction was observed between p-fluorophenyl ring and Glu357. Moreover, two hydrogen bonds were established; one of them between oxime OH group and Asn401 and the other between phenyl ring and Ile663. Whereas, compound **8c** showed pi-hydrogen bonds between sulfonamide nitrogen and Phe415 and, phenyl ring and Leu408. Arene-arene contacts were set up between 1,2,3-triazole ring and His361. Besides, formation of hydrogen bonds occurred between oxime nitrogen and Asn401 and, one of the pyrazole hydrogens and Ile 400 and one of the sulfonamide oxygens and Phe353 (Fig. 13).

For docking into COX-2 and 15-LOX enzymes, it should be pointed out that the binding poses of triazolyl thiazoles (**5a** over **5d**) or the triazolyl pyrazoles (**8b** over **8c**) were almost superimposable on one another, as shown in Fig. 14 as a representative example.

Molecular docking experiment of the sulfonamide derivative 5d into hCA II enzyme (PDB code: 5LJT) and hCA XII (PDB code: 1JDO), showed that it lied deeply into the active sites of both enzymes. They were bound to neighboring amino acids in a classical mode for sulfonamide zinc binder carbonic anhydrase inhibitors (Figs. 15 and 16). In detail, the nitrogen atom of the sulfonamide group bonded directly to the zinc atom of CA II (distance  $\approx 2 \text{ Å}$ ) distorting the tetrahedron Zn coordination. Furthermore, an extra ionic contact occurred between one of sulfonamide oxygen and Zn atom. Also, the other sulfonamide oxygen participated in hydrogen bond (distance  $\approx 2.9$  Å) with the backbone nitrogen atom of Thr199. Moreover, more contacts were observed in case of hCA XII enzyme such as pi-hydrogen interaction between p-sulfonamidophenyl ring and Leu198 in addition to hydrogen bond formed between the latter ring and Thr200. Also, hydrogen bond was established between oxygen atom of sulfonamide group and Thr200.

To sum up, the best-docked poses of compounds **5a, 5d, 8b and 8c** in the active sites of COX-2, 15-LOX, hCA II and hCA XII enzymes showed that most of the interactions adopted by these compounds were shared with **S58, RS7, A6N and AZM** crystal structures (refer to Figures **SM1-SM4**, supporting information for interactions of crystal structures), respectively. For COX-2 enzyme, these key interactions were exemplified by Arg120, Tyr355, Leu352 and Ser353 and Val523. Whereas for 15-LOX enzyme, all the compounds occupied the U-shaped hydrophobic channel formed by side chains of hydrophobic amino acids Phe175, Phe353, Leu362, Phe415, Met419, Ile593 and Leu597 in addition to arene-arene interaction

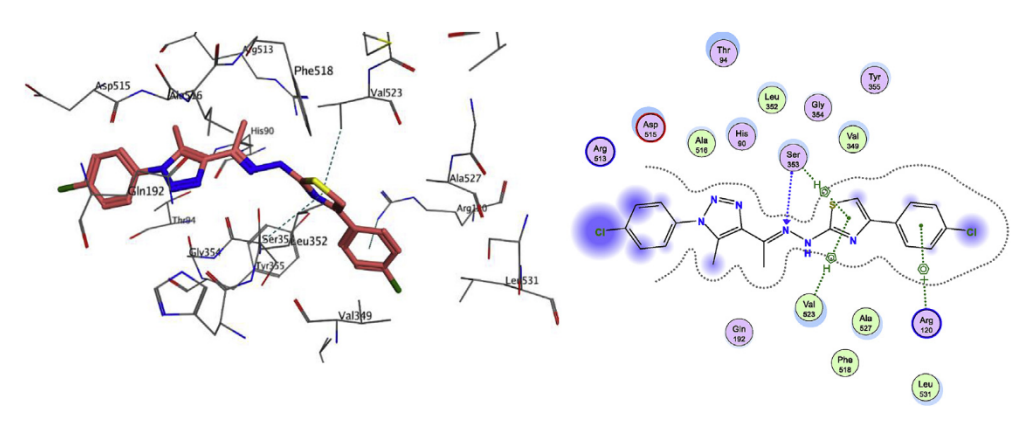


Fig. 6. Docking and binding pattern of compound 5a into COX-2 active site (PDB 1CX2) in 3D (left panel), 2D (right panel) views.

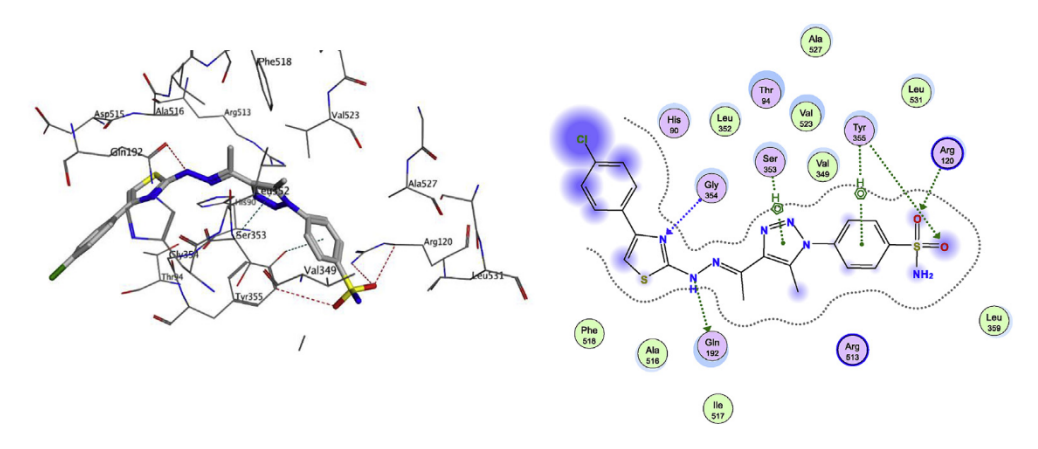


Fig. 7. Docking and binding pattern of compound 5d into COX-2 active site (PDB 1CX2) in 3D (left panel), 2D (right panel) views.

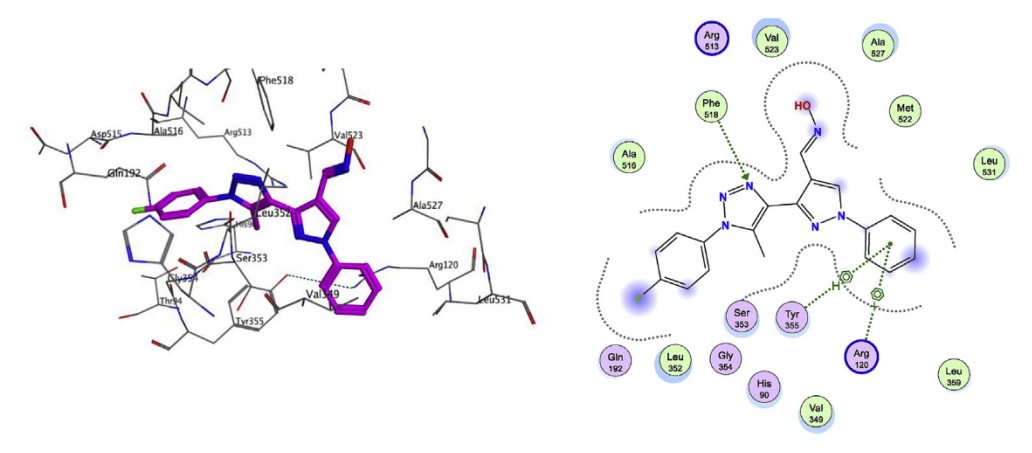


Fig. 8. Docking and binding pattern of compound 8b into COX-2 active site (PDB 1CX2) in 3D (left panel), 2D (right panel) views.

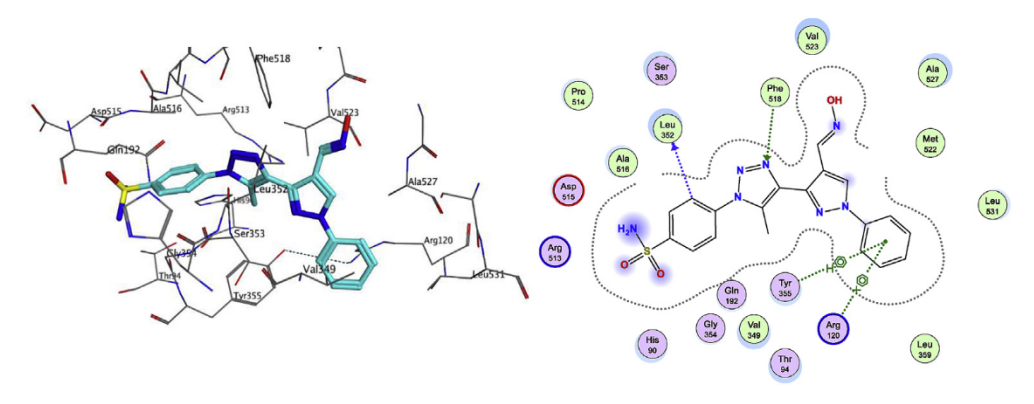


Fig. 9. Docking and binding pattern of compound 8c into COX-2 active site (PDB 1CX2) in 3D (left panel), 2D (right panel) views.

with His361 (for **8c**). For hCA II and hCA XII enzymes, **5d** showed the same interaction patterns as **A6N** (for hCA II) and **AZM** (for hCA XII) where the sulfonamide nitrogen anchor zinc atom in addition to binding with the key amino acids Thr199 and Leu198 (for hCA II) and Thr199, Thr200 and Leu198 (for hCA XII).

## 2.4. In silico prediction of physicochemical properties, drug likeness, pharmacokinetic profile and ligand efficiency metrics

Early determination of physicochemical and pharmacokinetic characters is of paramount importance in drug development programs as it can dramatically enhance the efficiency of lead optimization step [53].

Accordingly, *in silico* physicochemical properties, drug likeness and pharmacokinetic parameters of the most active compounds **5a**, **5d**, **8b** and **8c** were predicted by FAF-drugs4 online server [54,55], Pre-ADMET [56] and Datawarrior software [57] (Table 7). They showed good oral bioavailability in light of Lipinski's rule of five, Veber and Egan rules [58–60]. Compounds **5a** and **8b** showed medium Caco-2 permeability while **5d** and **8c** showed low Caco-2 permeability. The four compounds exhibited low MDCK permeability and high percentage of intestinal absorption. A positive

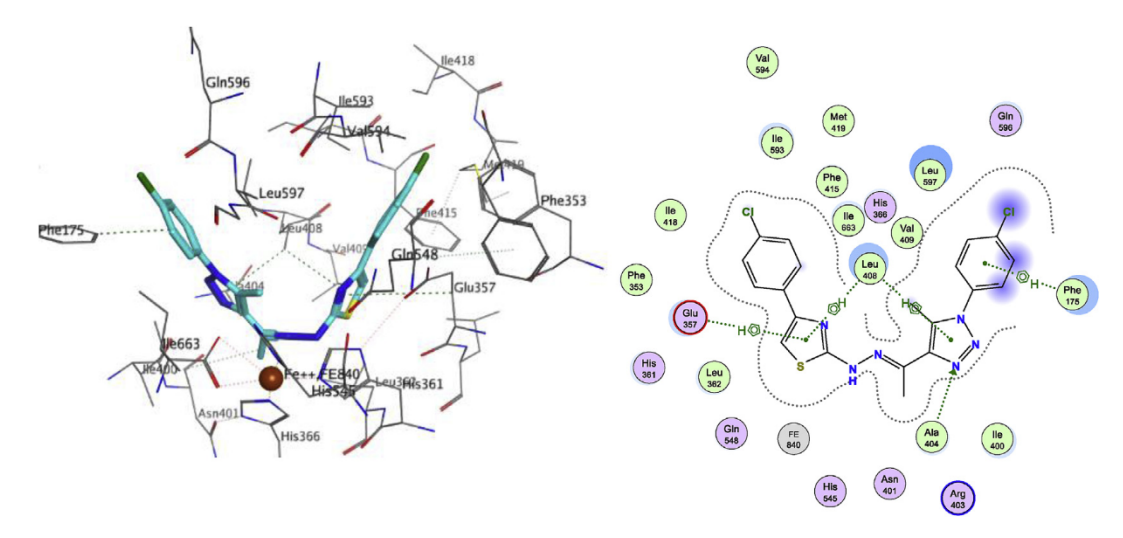


Fig. 10. Docking and binding pattern of compound 5a into 15-LOX active site (PDB 1LOX) in 3D (left panel), 2D (right panel) views.

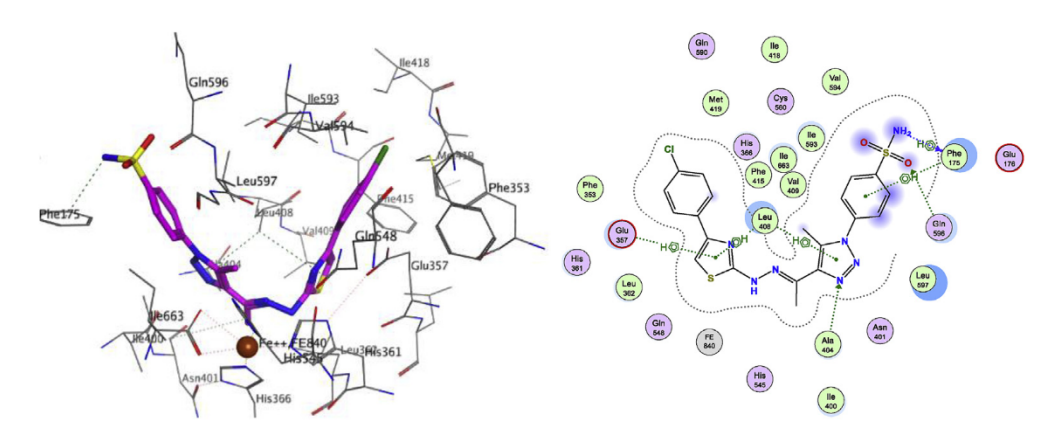


Fig. 11. Docking and binding pattern of compound 5d into 15-LOX active site (PDB 1LOX) in 3D (left panel), 2D (right panel) views.

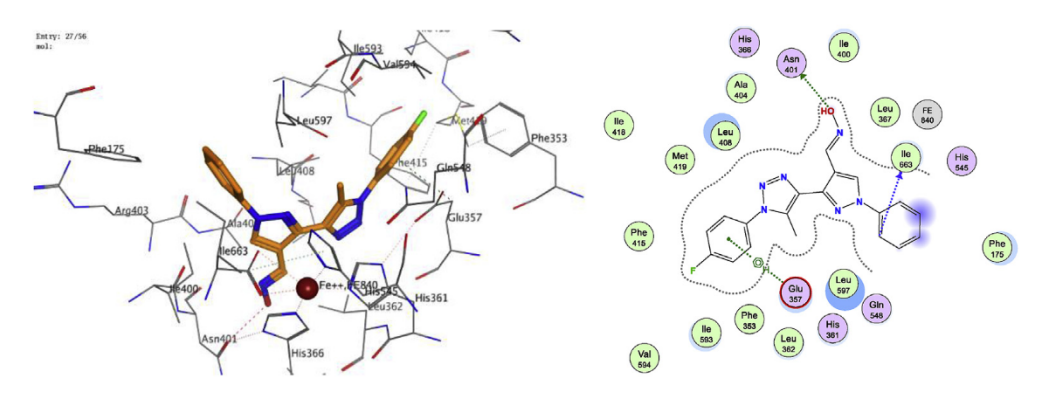


Fig. 12. Docking and binding pattern of compound 8b into 15-LOX active site (PDB 1LOX) in 3D (left panel), 2D (right panel) views.

drug-likeness score was predicted for compounds **5d** and **8c** whereas those for compounds **5a** and **8b** were negative. No PAINs were detected indicating genuine activity. The structural alerts are of low risk making the compounds of intermediate toxicity.

Other metrics, relating ligand's potency to its physicochemical properties, such as ligand efficiency (LE) and lipophilic ligand efficiency (LLE), have been devised. The former dictates if molecular size is responsible for potency while the latter employs lipophilicity [61].

LE values of the four compounds regarding the three studied enzymes, ranged from 0.25 to 0.37 which conform to the approved minimum LE either for lead compounds (around 0.3) or more than 0.3 for drug candidates [62,63]. Moreover, LLE values for both COX-2 and 15-LOX inhibitory activities for compounds **8b** and **8c**, as well as the values for hCA XII inhibition for compounds **5d** and **8c**, shown in Table 7, varied from 3.08 to 6.18, which agree with the cutoff standard values either for lead compounds ( $\geq$ 3) or drug candidates ( $\geq$ 5) [63]. Intriguingly, the aforementioned *in silico* 

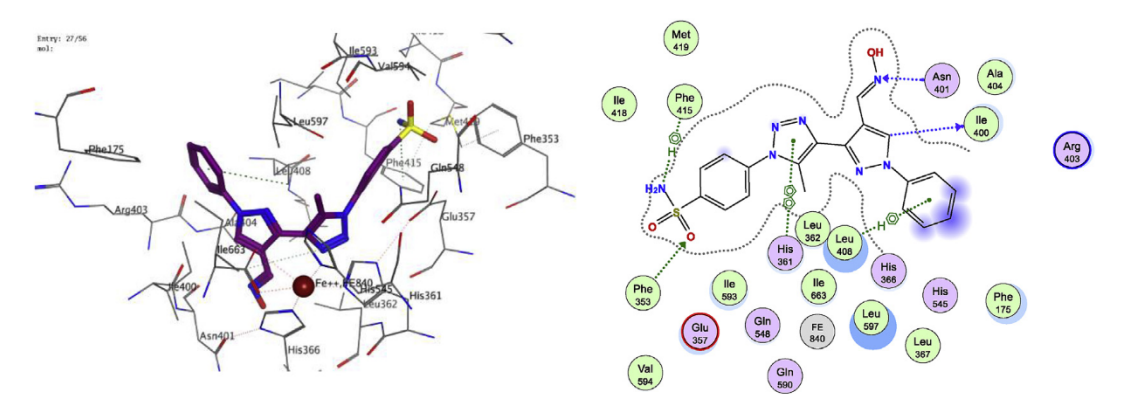
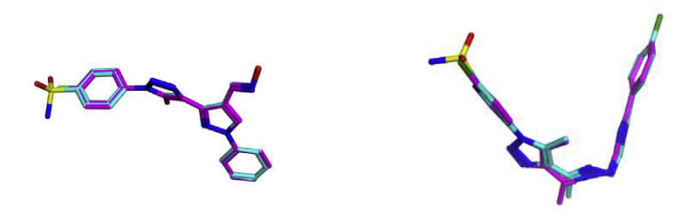


Fig. 13. Docking and binding pattern of compound 8c into 15-LOX active site (PDB 1LOX) in 3D (left panel), 2D (right panel) views.



**Figure 14.** 3D diagram for overlaid docking poses of **8b** (fuchsia) and **8c** (cyan) in COX-2 active site (PDB code: 1CX2) (left panel) and for overlaid docking poses of **5a** (cyan) and **5d** (fuchsia) in 15-LOX active site (PDB code: 1LOX) (right panel).

predictions verified the convenience of these compounds as lead-like candidates.

### 3. Conclusions

In order to tackle cancer via modulating different molecular targets, we designed 1,2,3-triazole-based molecular frameworks that would simultaneously inhibit COX-2, 15-LOX and tumor associated carbonic anhydrase enzymes. We envisioned that such MTDLs would be more powerful tools to combat the complex multifaceted nature of cancer. The synthesized compounds based

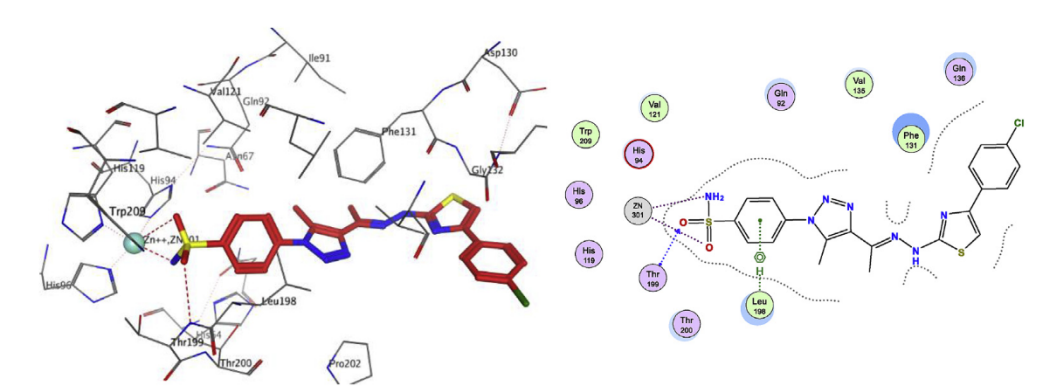
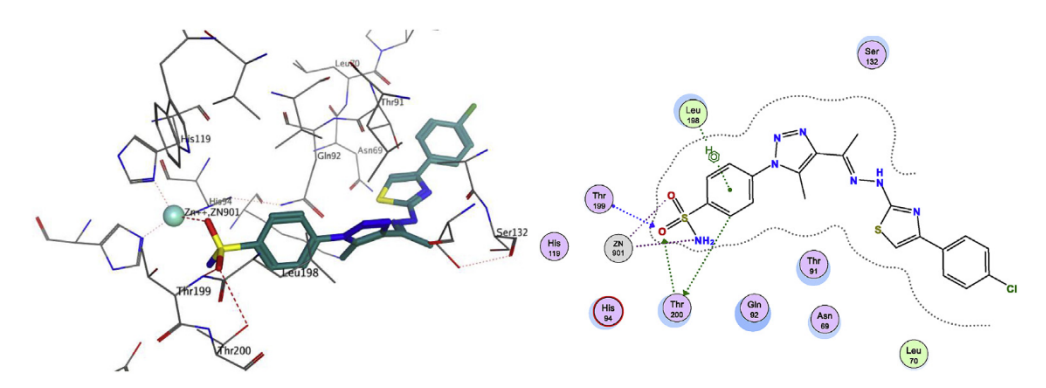


Fig. 15. Docking and binding pattern of compound 5d into hCA II active site (PDB 5LJT) in 3D (left panel, hydrogen bond appear as red dots and Zn atom appear as cyan sphere), 2D (right panel) views. (For interpretation of the references to color in this figure legend, the reader is referred to the Web version of this article.)



**Fig. 16.** Docking and binding pattern of compound **5d** into hCA XII active site (PDB 1JD0) in 3D (left panel, hydrogen bond appear as red dots and Zn atom appear as cyan sphere), 2D (right panel) views. (For interpretation of the references to color in this figure legend, the reader is referred to the Web version of this article.)

**Table 7** *In silico* physicochemical properties, ADME and ligand efficiency data of compounds **5a**, **5d**, **8b** and **8c**.

	5a	5d	8b	8c
LogP <sup>a,b</sup>	6.2	4.14	3.23	1.7
M.wt <sup>a,c</sup>	443.35	487.99	362.36	423.45
tPSA <sup>a,d</sup>	96.23	164.77	83.95	152.49
NROTB <sup>a,e</sup>	5	6	4	5
HBD <sup>a,f</sup>	1	3	1	3
HBA <sup>a,g</sup>	6	9	7	10
Lipinski violation <sup>a,h</sup>	1	0	0	0
Drug likeness	-0.24	1.82	-2.33	0.98
Solubility <sup>a,i</sup>	659.84	2229.49	5193.9	12129.84
VEBER oral bioavailability <sup>a,j</sup>	Good	Good	Good	Good
EGAN oral bioavailability <sup>a,k</sup>	Good	Good	Good	Good
Caco-2 <sup>l,m</sup>	31.1	0.5	13.8	0.7
MDCK <sup>l,n</sup>	0.2	0.12	0.7	1.7
HIA <sup>l,o</sup>	96.9	96.9	96.4	94.7
PAINs detection <sup>a,p</sup>	0	0	0	0
Structural alerts <sup>a,q</sup>	Low risk halogenure	Low risk halogenure	Low risk halogenure	Low risk oxime
	Low risk hydrazone	Low risk hydrazone	Low risk oxime	
Result	intermediate	intermediate	intermediate	intermediate
LE <sup>r</sup> (COX-2)	0.34	0.32	0.37	0.34
LLE <sup>s</sup>	0.62	2.58	4.74	6.18
LE (15-LOX)	0.27	0.25	0.29	0.27
LLE	-0.86	1.08	3.17	4.69
LE (hCA XII)	-	0.34	-	0.31
LLE	-	3.08	-	5.61

- <sup>a</sup> Physicochemical properties predicted by FAF-drugs4 server.
- <sup>b</sup> Octanol-water partition coefficient predictor by XLOGP3 method.
- <sup>c</sup> Molecular weight.
- d Topological polar surface area.
- e Number of rotatable bonds.
- f Number of H-bond donors.
- g Number of H-bond acceptors.
- <sup>h</sup> Lr. Lipinski Rule violation ( $\log P \le 5$ , H-bond donors  $\le 5$ , H-bond acceptors  $\le 10$ , and a molecular weight  $\le 500$ ).
- i Solubility in mg/L.
- <sup>j</sup> Veber rule (rotatable bonds <10, tPSA <140).
- k Egan rule (tPSA <132 and -1<logP <6).
- <sup>1</sup> Physicochemical properties predicted by Pre-ADMET.
- m Apparent Caco-2 permeability (nm/sec) Permeability through cells derived from human colon adenocarcinoma; < 4 nm/sec (low permeability), values from 4 to 70 nm/sec (medium permeability) and > 70 nm/sec (high permeability).
- <sup>n</sup> Apparent MDCK permeability (nm/sec) Permeability through Madin—Darby canine kidney cells; < 25 nm/sec (low permeability), values from 25 to 500 nm/sec (medium permeability) and > 500 nm/sec (high permeability).
- <sup>o</sup> Human intestinal absorption %; values from 0 to 20% (poorly absorbed), values from 20 to 70% (moderately absorbed) and values from 70 to 100% (well absorbed).
- P Pan Assay Interference Compounds are compounds that appear as frequent hitters (promiscuous compounds) in many biochemical high throughput screens.
- q Undesirable moieties and substructures involved in toxicity problems; intermediate means low-risk structural alerts with a number of occurrences below the threshold.
- r Ligand efficiency.
- <sup>s</sup> Lipophilic ligand efficiency.

on our design, were challenged in vitro at the abovementioned molecular targets. The four compounds 5a, 5d, 8b and 8c have been identified as both highly potent COX-2 inhibitors (IC50 ranging from 0.04 to  $0.06~\mu\text{M},$  COX-2 SI from 198 to 310), and moderately potent 15-LOX inhibitors (IC50 ranging from 1.29 to 1.98  $\mu$ M). COX-2 inhibitory activity was confirmed in tumor cell-based model. Interestingly, compounds 5d and 8c were capable of inhibiting the tumor associated isoform hCA XII in low (Ki 13.4 nM) and medium (Ki 154.4 nM) nanomolar ranges, respectively. Moreover, results of in vitro antiproliferative activities on cancer cell lines showed that compound 5a inhibited the growth of A549, HepG2 and MCF7 cells with single digit micromolar IC<sub>50</sub> values (2.37–8.9  $\mu$ M) while its sulfonamide congener 5d was moderately active on A549 cells (28.5 μM IC<sub>50</sub> value). Compounds **8b** and **8c** possessed significant inhibitory activity on MCF7 cells (5.32 and 3.2 μM, respectively). Significantly, CA inhibitory activity of **5d** afforded an enhanced cytotoxic activity against HT-29, with a high level of basal CA expression, compared to other cell lines with low or no basal expression. Besides, flow cytometric cell cycle analysis confirmed compounds 5a and 5d to both arrest G2/M cell growth and trigger apoptosis. They effectively increased the expression levels of caspase-9 and the proapoptotic protein Bax and at the same time, downregulated that of the antiapoptotic protein Bcl-2. Compound **8c** reduced tumor size in an *in vivo* cancer xenograft model. Molecular docking experiments of the most active compounds on the three targets substantiated their *in vitro* inhibitory activities, highlighting essential binding interactions. Appropriate *In silico* predictions and ligand efficiency indices provided additional support for their lead-like characters. Hence, these compounds demonstrated their structural convenience to advance to further optimization cycles as potential multi-target anticancer agents.

### 4. Experimental

### 4.1. Chemistry

All chemicals were purchased from commercial sources and directly used without purification. Melting points were determined in open-glass capillaries on Stuart Scientific melting point apparatus (SMP10) and are uncorrected. Follow up of the reactions' rates was performed by thin-layer chromatography (TLC) on silica gel pre-coated Merck aluminum GF254 plates, and the spots were visualized by exposure to iodine vapors or UV-lamp at  $\lambda$  254 nm for few seconds. Infrared spectra (IR) were recorded, using KBr discs,

on a PerkinElmer 1430 infrared spectrophotometer at Institute of Graduate Studies and Research, Alexandria University. Proton nuclear magnetic resonance spectra (<sup>1</sup>H NMR) were scanned on Bruker Avance III 400 MHz spectrometer. Data were analyzed using MestRe-C and Topspin 3.1 software at NMR unit at the Faculty of Pharmacy, Beni Suef University and at the microanalytical unit, Faculty of Pharmacy, Cairo University using deuterated dimethylsulfoxide (DMSO- $d_6$ ) as a solvent. Data were recorded as chemical shifts expressed in  $\delta$  values (ppm) relative to tetramethylsilane (TMS) as internal standard. The type of signal splitting was indicated by one of the following letters: s = singlet, d = doublet, t = triplet, q = quartet, dd = doublet of doublet and m= multiplet.  $^{13}C$  NMR spectra were scanned on Bruker spectrometer (100 MHz) at Center for Clinical Pharmacology, Washington University, School of Medicine. High resolution mass spectra were run on Bruker 10 T APEX-Qe FTICR-MS at the College of Science Major Instrumentation Cluster (COSMIC) LAB, Old Dominion University, Norfolk, Virginia. Electrospray ionization mass spectra (ESI-MS) were run on liquid chromatograph/mass spectrometer Agilent 1100 LC/MS at Center for Clinical Pharmacology, Washington University, School of Medicine. Electron impact mass spectra (EIMS) were carried out using direct inlet unit (DI-50) in the Shimadzu QP-5050 GC-MS at the Regional Center for Mycology and Biotechnology, Al-Azhar University. Checking purity of the new compounds was performed by elemental analyses (C, H, N and S) using FLASH 2000 CHNS/O analyzer, Thermo Scientific at the Regional Center for Mycology and Biotechnology (RCMB), Al-Azhar University. The results were within  $\pm 0.4\%$  of the calculated values for the proposed formulae. Compounds were named based on the naming algorithm developed by CambridgeSoft Corporation and used in ChemDraw Professional 16.0.1.4. Aryl azides (1a-e) [64] and compounds **2a** [65], **2b** [66], **4a** [67], **5a** [68], **6a** and **7a** [33] were prepared as previously reported.

### 4.1.1. General procedure for the synthesis of compounds 2a-e

A mixture of the appropriate aryl azide (1a-e) (5 mmol) and acetylacetone (0.65 g, 0.64 ml, 5 mmol) was added to sodium methoxide solution (7.5 mmol, prepared from 0.17 g of sodium and 10 ml of methanol). The mixture was stirred at room temperature overnight until a precipitate was formed. For derivatives 2c-e, the precipitate was washed with dil. HCl then dried and crystallized from aqueous ethanol.

4.1.2. 4-(4-Acetyl-5-methyl-1H-1,2,3-triazol-1-yl)benzoic acid (**2c**) Off white powder; yield 63%, m.p. 244–246 °C. IR (KBr, cm<sup>-1</sup>): 1699 (C=O carboxylic acid), 1682 (C=O), 1553 (C=C).  $^{1}$ H NMR (400 MHz, DMSO- $^{4}$ G):  $\delta$  2.57 (s, 3H, COCH<sub>3</sub>), 2.65 (s, 3H, CH<sub>3</sub>), 7.77 (d,  $^{1}$ J = 8.4 Hz, 2H, phenyl-C<sub>3,5</sub>-H), 8.18 (d,  $^{1}$ J = 8.4 Hz, 2H, phenyl-C<sub>2,6</sub>-H).  $^{13}$ C NMR (100 MHz, DMSO- $^{4}$ G):  $\delta$  10.3, 28.2, 125.8, 131.1, 133.4, 138.3, 138.5, 143.5, 167, 193.8. ESI-MS  $^{1}$ Mz: 246.1 [M<sup>++</sup>+1], 244.1 [M<sup>+-</sup>-1]. Anal. Calcd for  $^{1}$ C<sub>12</sub>H<sub>11</sub>N<sub>3</sub>O<sub>3</sub> (245.23) C, 58.77; H, 4.52; N, 17.13. Found: C, 58.95; H, 4.78; N, 17.29.

### 4.1.3. 4-(4-Acetyl-5-methyl-1H-1,2,3-triazol-1-yl) benzenesulfonamide (**2d**)

Buff powder; yield 66%, m.p. 222–224 °C. IR (KBr, cm $^{-1}$ ): 3358, 3284 (NH<sub>2</sub>), 1689 (C=O), 1554 (C=C), 1359, 1168 (SO<sub>2</sub>). <sup>1</sup>H NMR (400 MHz, DMSO- $d_6$ ):  $\delta$  2.58 (s, 3H, COCH<sub>3</sub>), 2.66 (s, 3H, CH<sub>3</sub>), 7.62 (s, 2H, NH<sub>2</sub>, D<sub>2</sub>O exchangeable), 7.89 (d, J = 8.4 Hz, 2H, phenyl-C<sub>2,6</sub>-H), 8.08 (d, J = 8.4 Hz, 2H, phenyl-C<sub>3,5</sub>-H). <sup>13</sup>C NMR (100 MHz, DMSO- $d_6$ ):  $\delta$  10.2, 28.2, 126.5, 127.7, 137.8, 138.5, 143.5, 145.8, 194. ESI-MS m/z: 281 [M $^+$ +1], 279 [M $^+$ -1]. Anal. Calcd for C<sub>11</sub>H<sub>12</sub>N<sub>4</sub>O<sub>3</sub>S (280.30) C, 47.13; H, 4.32; N, 19.99; S, 11.44. Found: C, 47.32; H, 4.59; N, 20.16; S, 11.58.

4.1.3.1. 4-(4-Acetyl-5-methyl-1H-1,2,3-triazol-1-yl)-N-(thiazol-2-yl) benzenesulfonamide (2e). Light brown powder; yield 70%, m.p. 212–213 °C. IR (KBr, cm<sup>-1</sup>): 3458 (NH), 1684 (C=O), 1540 (C=C), 1311, 1148 (S=O). <sup>1</sup>H NMR (400 MHz, DMSO- $d_6$ ):  $\delta$  2.56 (s, 3H, COCH<sub>3</sub>), 2.65 (s, 3H, CH<sub>3</sub>), 6.90 (d, J = 4.8 Hz, 1H, thaizolyl-C<sub>5</sub>-H), 7.30 (d, J = 4.8 Hz, 1H, thaizolyl-C<sub>4</sub>-H), 7.84 (d, J = 8.4 Hz, 2H, phenyl-C<sub>2,6</sub>-H), 8.05 (d, J = 8.4 Hz, 2H, phenyl-C<sub>3,5</sub>-H). <sup>13</sup>C NMR (100 MHz, DMSO- $d_6$ ):  $\delta$  10.3, 28.2, 109.2, 125.2, 126.4, 127.7, 138.0, 138.5, 143.5, 144.1, 169.7, 193.8. ESI-MS m/z: 364 [M<sup>++</sup>+1], 362 [M<sup>+-</sup>-1]. Anal. Calcd for C<sub>14</sub>H<sub>13</sub>N<sub>5</sub>O<sub>3</sub>S<sub>2</sub> (363.41) C, 46.27; H, 3.61; N, 19.27; S, 17.65. Found: C, 46.51; H, 3.87; N, 19.53; S, 17.51.

### 4.1.4. General procedure for the synthesis of compounds 3a-e

A solution of semicarbazide hydrochloride (0.22 g, 2 mmol) in 10 ml of water was added to a mixture of the appropriate ketone (2a-e) (2 mmol) and sodium acetate (0.2 g, 2.5 mmol) in ethanol (20 ml). The reaction mixture was refluxed for 8 h. After the reaction completion, the separated solids were filtered, washed with water, dried and crystallized from ethanol.

4.1.4.1. 2-[1-[1-(4-Chlorophenyl)-5-methyl-1H-1,2,3-triazol-4-yl] ethylidene]hydrazine-1-carboxamide (3a). White powder; yield 55%, m.p. 272–273 °C. IR (KBr, cm $^{-1}$ ): 3486, 3179, 3159 (NH<sub>2</sub>, NH), 1755 (C=O), 1654 (C=N), 1589 (C=C). <sup>1</sup>H NMR (400 MHz, DMSO-d<sub>6</sub>):  $\delta$  2.36 (s, 3H, CH<sub>3</sub>–C=N), 2.48 (s, 3H, CH<sub>3</sub>), 6.30 (s, 2H, NH<sub>2</sub>, D<sub>2</sub>O exchangeable), 7.64 (d, J = 8.4 Hz, 2H, phenyl-C<sub>3,5</sub>-H), 7.72 (d, J = 8.4 Hz, 2H, phenyl-C<sub>2,6</sub>-H), 9.48 (s, 1H, NH, D<sub>2</sub>O exchangeable). ESI-MS m/z: 293.1 [M $^{++}$ +1]. Anal. Calcd for C<sub>12</sub>H<sub>13</sub>ClN<sub>6</sub>O (292.72) C, 49.24; H, 4.48; N, 28.71. Found: C, 49.52; H, 4.67; N, 28.57.

4.1.4.2. 2-[1-[1-(4-Fluorophenyl)-5-methyl-1H-1,2,3-triazol-4-yl] ethylidene]hydrazine-1-carboxamide (**3b**). White powder; yield 52%, blackens at 211 °C and melts >300 °C. IR (KBr, cm<sup>-1</sup>): 3486, 3179, 3153 (NH<sub>2</sub>, NH), 1752 (C=O), 1654 (C=N), 1590 (C=C). <sup>1</sup>H NMR (400 MHz, DMSO- $d_6$ ): δ 2.36 (s, 3H, CH<sub>3</sub>-C=N), 2.46 (s, 3H, CH<sub>3</sub>), 6.36 (s, 2H, NH<sub>2</sub>, D<sub>2</sub>O exchangeable), 7.47-7.51 (m, 2H, phenyl-C<sub>3,5</sub>-H), 7.65-7.68 (m, 2H, phenyl-C<sub>2,6</sub>-H), 9.53 (s, 1H, NH, D<sub>2</sub>O exchangeable). <sup>13</sup>C NMR (100 MHz, DMSO- $d_6$ ): δ 11.0, 14.4, 116.4, 128.4, 131.9, 132.5, 141.0, 143.4, 157.8, 161.5. ESI-MS m/z: 277.1 [M<sup>++</sup>+1]. Anal. Calcd for C<sub>12</sub>H<sub>13</sub>FN<sub>6</sub>O (276.27) C, 52.17; H, 4.74; N, 30.42. Found: C, 52.49; H, 4.85; N, 30.18.

4.1.4.3. 4-[4-[1-(2-Carbamoylhydrazineylidene)ethyl]-5-methyl-1H-1,2,3-triazol-1-yl]benzoic acid (**3c**). White powder; yield 53%, m.p. > 300 °C. IR (KBr, cm<sup>-1</sup>): 3479 (OH), 3256, 3144 (NH<sub>2</sub>, NH), 1751 (C= O), 1693 (C=O acid), 1593 (C=N). <sup>1</sup>H NMR (400 MHz, DMSO- $d_6$ ):  $\delta$  2.37 (s, 3H, CH<sub>3</sub>-C=N), 2.53 (s, 3H, CH<sub>3</sub>), 6.30 (s, 2H, NH<sub>2</sub>, D<sub>2</sub>O exchangeable), 7.74 (d, J = 8 Hz, 2H, phenyl-C<sub>3,5</sub>-H), 8.18 (d, J = 8 Hz, 2H, phenyl-C<sub>2,6</sub>-H), 9.50 (s, 1H, NH, D<sub>2</sub>O exchangeable). <sup>13</sup>C NMR (100 MHz, DMSO- $d_6$ ):  $\delta$  11.2, 14.5, 125.7, 131.2, 132.5, 132.5, 139.3, 140.9, 143.4, 157.5, 166.9. ESI-MS m/z: 303.1 [M<sup>++</sup>+1], 301.1 [M<sup>++</sup>-1]. Anal. Calcd for C<sub>13</sub>H<sub>14</sub>N<sub>6</sub>O<sub>3</sub> (302.29) C, 51.65; H, 4.67; N, 27.80. Found: C, 51.88; H, 4.81; N, 28.09.

4.1.4.4. 2-[1-[5-Methyl-1-(4-sulfamoylphenyl)-1H-1,2,3-triazol-4-yl] ethylidene]hydrazine-1-carboxamide (3d). White powder; yield 51%, m.p. 252–253 °C. IR (KBr, cm<sup>-1</sup>): 3348 (NH), 3362, 3266 (NH<sub>2</sub>), 1752 (C=O), 1692 (C=N), 1585 (C=C), 1308, 1161 (SO<sub>2</sub>). ¹H NMR (400 MHz, DMSO- $d_6$ ):  $\delta$  2.37 (s, 3H, CH<sub>3</sub>–C=N), 2.53 (s, 3H, CH<sub>3</sub>), 6.30 (s, 2H, NH<sub>2</sub>, D<sub>2</sub>O exchangeable), 7.60 (s, 2H, SO<sub>2</sub>NH<sub>2</sub>, D<sub>2</sub>O exchangeable), 7.83–7.93 (m, 2H, phenyl-C<sub>3,5</sub>-H), 8.06–8.1 (m, 2H, phenyl-C<sub>2,6</sub>-H), 9.50 (s, 1H, NH, D<sub>2</sub>O exchangeable). <sup>13</sup>C NMR (100 MHz, DMSO- $d_6$ ):  $\delta$  11.3, 14.5, 126.5, 127.7, 134.8, 138.4, 140.9, 143.2, 145.5, 157.6. ESI-MS m/z: 336.0 [M<sup>+-</sup>-1]. Anal. Calcd for

C<sub>12</sub>H<sub>15</sub>N<sub>7</sub>O<sub>3</sub>S (337.36) C, 42.72; H, 4.48; N, 29.06; S, 9.50. Found: C, 42.96; H, 4.69; N, 28.87; S, 9.43.

4.1.4.5. 2-[1-[5-Methyl-1-(4-(N-(thiazol-2-yl)sulfamoyl)phenyl)-1H-1,2,3-triazol-4-yl]ethylidene]hydrazine-1-carboxamide (3e). White powder; yield 48%, m.p. 260–263 °C. IR (KBr, cm $^{-1}$ ): 3359, 3411 (NH<sub>2</sub>, NH), 1694 (C=O), 1679 (C=N), 1574 (C=C), 1309, 1141 (S=O).  $^{1}$ H NMR (400 MHz, DMSO- $^{4}$ G):  $\delta$  2.36 (s, 3H, CH<sub>3</sub>–C=N), 2.52 (s, 3H, CH<sub>3</sub>), 6.29 (s, 2H, NH<sub>2</sub>, D<sub>2</sub>O exchangeable), 6.89 (d,  $^{1}$ J = 4.8 Hz, 1H, thiazolyl-C<sub>5</sub>-H), 7.31 (d,  $^{1}$ J = 4.8 Hz, 1H, thiazolyl-C<sub>4</sub>-H), 7.77 (d,  $^{1}$ J = 8 Hz, 2H, phenyl-C<sub>3,5</sub>-H), 8.02 (d,  $^{1}$ J = 8 Hz, 2H, phenyl-C<sub>2,6</sub>-H), 9.49 (s, 1H, NH, D<sub>2</sub>O exchangeable), 12.91 (s, 1H, SO<sub>2</sub>NH, D<sub>2</sub>O exchangeable).  $^{13}$ C NMR (100 MHz, DMSO- $^{1}$ G):  $\delta$  11.2, 14.5, 109.2, 125.2, 126.2, 126.4, 127.7, 132.5, 138.6, 140.8, 143.4, 143.8, 157.4, 169.7. EI-MS  $^{1}$ M/z: 420.93 [M $^{+}$ +1]. Anal. Calcd for C<sub>15</sub>H<sub>16</sub>N<sub>8</sub>O<sub>3</sub>S<sub>2</sub> (420.47) C, 42.85; H, 3.84; N, 26.65; S, 15.25. Found: C, 43.09; H, 3.97; N, 26.81; S, 15.49.

### 4.1.5. General procedure for the synthesis of compounds 4a-e

A mixture of the appropriate ketone (2a and 2c-e) (5 mmol) and thiosemicarbazide (0.46 g, 5 mmol) was refluxed in glacial acetic acid (15 ml) for 8-12 h, then left to cool, poured onto ice water. The formed precipitate was filtered and dried. The product was then crystallized from ethanol.

For **4b**, an equimolar mixture of **2b** and thiosemicarbazide was fused at 180 °C for 20 min, left to cool, triturated with ethanol, filtered, dried and crystallized from ethanol.

4.1.5.1. 2-[1-[1-(4-Fluorophenyl)-5-methyl-1H-1,2,3-triazol-4-yl]ethylidene]hydrazine-1-carbothioamide (4b). White powder; yield 67%, m.p. 218–220 °C. IR (KBr, cm $^{-1}$ ): 3450 (NH), 3273, 3176 (NH $_2$ ), 1585 (C=N), 1507 (C=C), 1269 (C=S).  $^{1}$ H NMR (400 MHz, DMSO- $^{4}$ 6):  $\delta$  2.48 (s, 3H, CH $_3$ –C=N), 2.49 (s, 3H, CH $_3$ ), 7.35 and 8.37 (s, 2H, NH $_2$ , D $_2$ 0 exchangeable), 7.48–7.52 (m, 2H, phenyl-C $_3$ ,5-H), 7.64–7.68 (m, 2H, phenyl-C $_2$ ,6-H), 10.45 (s, 1H, C=N–NH, D $_2$ 0 exchangeable).  $^{13}$ C NMR (100 MHz, DMSO- $^{4}$ 6):  $\delta$  11.2, 15.1, 117.17, 128.2, 132.4, 133.6, 142.6, 145.2, 161.7, 179.5. ESI-MS  $^{m}$ / $^{z}$ : 293.1 [M $^{++}$ +1], 291.1 [M $^{+-}$ -1]. Anal. Calcd for C $_{12}$ H $_{13}$ FN $_6$ S (292.34) C, 49.30; H, 4.48; N, 28.75; S, 10.97. Found: C, 49.56; H, 4.63; N, 28.94; S, 11.24.

4.1.5.2. 4-[4-[1-(2-Carbamothioylhydrazineylidene)ethyl]-5-methyl-1H-1,2,3-triazol-1-yl]benzoic acid (4c). White powder; yield 67%, m.p. 276–278 °C. IR (KBr, cm $^{-1}$ ): 3500 (OH), 3436 (NH), 3297, 3152 (NH<sub>2</sub>), 1688 (C=O), 1575 (C=N), 1503 (C=C), 1285 (C=S).  $^{1}$ H NMR (400 MHz, DMSO- $d_6$ ):  $\delta$  2.50 (s, 3H, CH<sub>3</sub>–C=N), 2.54 (s, 3H, CH<sub>3</sub>), 7.37 and 8.39 (s, 2H, NH<sub>2</sub>, D<sub>2</sub>O exchangeable), 7.74 (d, J = 8.4 Hz, 2H, phenyl-C<sub>3,5</sub>-H), 8.18 (d, J = 8.4 Hz, 2H, phenyl-C<sub>2,6</sub>-H), 10.44 (s, 1H, C=N–NH, D<sub>2</sub>O exchangeable), 13.34 (s, 1H, COOH, D<sub>2</sub>O exchangeable).  $^{13}$ C NMR (100 MHz, DMSO- $d_6$ ):  $\delta$  11.4, 15.2, 125.8, 131.2, 132.3, 133.5, 139.3, 143.0, 145.0, 166.8, 179.5. ESI-MS m/z: 317.1 [M $^{+-}$ -1]. Anal. Calcd for C<sub>13</sub>H<sub>14</sub>N<sub>6</sub>O<sub>2</sub>S (318.35) C, 49.05; H, 4.43; N, 26.40; S, 10.07. Found: C, 49.32; H, 4.59; N, 26.23; S, 10.16.

4.1.5.3. 2-[1-[5-Methyl-1-(4-sulfamoylphenyl)-1H-1,2,3-triazol-4-yl] ethylidene]hydrazine-1-carbothioamide (4d). White powder; yield 67%, m.p. 218—221 °C. IR (KBr, cm $^{-1}$ ): 3466 (NH), 3346, 3128 (NH<sub>2</sub>), 1600 (C=N), 1501 (C=C), 1272 (C=S), 1350, 1164 (SO<sub>2</sub>). ¹H NMR (400 MHz, DMSO- $d_6$ ):  $\delta$  2.50 (s, 3H, CH<sub>3</sub>—C=N), 2.54 (s, 3H, CH<sub>3</sub>), 7.37 and 8.39 (s, 2H, NH<sub>2</sub>, D<sub>2</sub>O exchangeable), 7.60 (s, 1H, SO<sub>2</sub>NH<sub>2</sub>, D<sub>2</sub>O exchangeable), 7.83 (d, J = 8.4 Hz, 2H, phenyl-C<sub>3,5</sub>-H), 8.08 (d, J = 8.4 Hz, 2H, phenyl-C<sub>2,6</sub>-H), 10.45 (s, 1H, C=N-NH, D<sub>2</sub>O exchangeable).  $^{13}$ C NMR (100 MHz, DMSO- $d_6$ ):  $\delta$  11.4, 15.2, 126.4, 127.7, 133.6, 138.3, 143.0, 145.0, 145.5, 179.5. ESI-MS m/z: 352.0 [M $^{+}$ -1]. Anal. Calcd for C<sub>12</sub>H<sub>15</sub>N<sub>7</sub>O<sub>2</sub>S<sub>2</sub> (353.42) C, 40.78; H, 4.28; N, 27.74; S, 18.15. Found: C, 41.04; H, 4.37; N, 27.85; S, 18.07.

4.1.5.4. 2-[1-[5-Methyl-1-(4-(N-(thiazol-2-yl)sulfamoyl)phenyl)-1H-1,2,3-triazol-4-yl]ethylidene]hydrazine-1-carbothioamide (4e). White powder; yield 67%, m.p. 230–232 °C. IR (KBr, cm $^{-1}$ ): 3417 (NH), 3257, 3155 (NH<sub>2</sub>), 1510 (C=C), 1595 (C=N), 1275 (C=S), 1301, 1100 (S=O).  $^1\mathrm{H}$  NMR (400 MHz, DMSO- $d_6$ ):  $\delta$  2.48 (s, 3H, CH<sub>3</sub>–C=N), 2.53 (s, 3H, CH<sub>3</sub>), 6.90 (d, J=4.8 Hz, 1H, thiazolyl-C<sub>5</sub>-H), 7.31 (d, J=4.8 Hz, 1H, thiazolyl-C<sub>4</sub>-H), 7.39 and 8.39 (s, 2H, NH<sub>2</sub>, D<sub>2</sub>O exchangeable), 7.79 (d, J=8.4 Hz, 2H, phenyl-C<sub>3,5</sub>-H), 8.05 (d, J=8.4 Hz, 2H, phenyl-C<sub>2,6</sub>-H), 10.44 (s, 1H, C=N-NH, D<sub>2</sub>O exchangeable).  $^{13}\mathrm{C}$  NMR (100 MHz, DMSO- $d_6$ ):  $\delta$  11.4, 15.2, 109.2, 125.2, 126.3, 127.8, 133.6, 138.4, 143.0, 143.8, 145.0, 169.7, 179.5. ESI-MS m/z: 435.0 [M $^+$ -1]. Anal. Calcd for C<sub>15</sub>H<sub>16</sub>N<sub>8</sub>O<sub>2</sub>S<sub>3</sub> (436.53) C, 41.27; H, 3.69; N, 25.67; S, 22.04. Found: C, 41.50; H, 3.85; N, 25.84; S, 22.19.

### 4.1.6. General procedure for the synthesis of compounds **5a-e**

A mixture of the appropriate thiosemicarbazone (**4a-e**) (2 mmol), p-chlorophenacyl bromide (2 mmol, 0.47 g) and catalytic amount of triethylamine or pyridine (for **5b**) in ethanol (15 ml) was refluxed for 3–5 h, left to cool. The formed product was filtered, washed and dried. The separated solid was then crystallized from ethanol.

4.1.6.1. 4-(4-Chlorophenyl)-2-[2-[1-(1-(4-chlorophenyl)-5-methyl-1H-1,2,3-triazol-4-yl)ethylidene]hydrazineyl]thiazole (5a). White powder; yield 67%, m.p. 220–221 °C. IR (KBr, cm $^{-1}$ ): 3447 (NH), 1628 (C=N), 1565 (C=C), 724 (C-S-C). <sup>1</sup>H NMR (400 MHz, DMSO- $d_6$ ):  $\delta$  2.51 (s, 3H, CH<sub>3</sub>-C=N), 2.58 (s, 3H, CH<sub>3</sub>), 7.41 (s, 1H, thiazolyl-C<sub>5</sub>-H), 7.48 (d, J=8.4 Hz, 4-chlorophenyl-C<sub>3,5</sub>-H), 7.69–7.74 (m, 4H, triazolyl-4-chlorophenyl), 7.90 (d, J=8.4 Hz, 4-chlorophenyl-C<sub>2,6</sub>-H), 11.39 (s, 1H, NH, D<sub>2</sub>O exchangeable). <sup>13</sup>C NMR (100 MHz, DMSO- $d_6$ ):  $\delta$  11.3, 14.9, 105.3, 127.7, 129.1, 130.2, 130.3, 132.4, 132.7, 134.9, 135.0, 142.7, 150.1, 170.2. HRMS-ESI: Calcd for C<sub>20</sub>H<sub>16</sub>Cl<sub>2</sub>N<sub>6</sub>SNa [M+Na] $^+$  465.042642, Found: 465.042671. Anal. Calcd for C<sub>20</sub>H<sub>16</sub>Cl<sub>2</sub>N<sub>6</sub>S (443.35) C, 54.18; H, 3.64; N, 18.96; S, 7.23. Found: C, 54.37; H, 3.87; N, 19.20; S, 7.36.

4.1.6.2. 4-(4-Chlorophenyl)-2-[2-[1-(1-(4-fluorophenyl)-5-methyl-1H-1,2,3-triazol-4-yl)ethylidene]hydrazineyl]thiazole **(5b)**. White powder; yield 67%, m.p. 209–211 °C. IR (KBr, cm $^{-1}$ ): 3458 (NH), 1620 (C=N), 1556 (C=C), 679 (C=S-C).  $^{1}$ H NMR (400 MHz, DMSO- $d_6$ ):  $\delta$  2.51 (s, 3H, CH<sub>3</sub>-C=N), 2.56 (s, 3H, CH<sub>3</sub>), 7.40 (s, 1H, thiazolyl-C<sub>5</sub>-H), 7.47 (d, J = 8.4 Hz, 2H, 4-chlorophenyl-C<sub>3,5</sub>-H), 7.50–7.52 (m, 2H, 4-fluorophenyl-C<sub>3,5</sub>-H), 7.70–7.73 (m, 2H, 4-fluorophenyl-C<sub>2,6</sub>-H), 7.89 (d, J = 8.4 Hz, 2H, 4-chlorophenyl-C<sub>2,6</sub>-H), 11.39 (s, 1H, NH, D<sub>2</sub>O exchangeable).  $^{13}$ C NMR (100 MHz, DMSO- $d_6$ ):  $\delta$  11.2, 14.8, 105.3, 117.0, 124.0, 127.8, 128.4, 129.1, 132.4, 132.5, 132.8, 142.5, 149.7, 161.7, 170.2. ESI-MS m/z: 427.0 [M $^{++}$ +1]. Anal. Calcd for C<sub>20</sub>H<sub>16</sub>CIFN<sub>6</sub>S (426.90) C, 56.27; H, 3.78; N, 19.69; S, 7.51. Found: C, 56.13; H, 3.96; N, 19.87; S, 7.42.

4.1.6.3. 4-[4-[1-(2-(4-(4-Chlorophenyl)thiazol-2-yl)hydrazineylidene)ethyl]-5-methyl-1H-1,2,3-triazol-1-yl]benzoic acid (5c). Creamy powder; yield 67%, m.p. 291–293 °C. IR (KBr, cm $^{-1}$ ): 3448 (NH, OH), 1691 (C=O), 1630 (C=N), 15,836 (C=C), 695 (C-S-C).  $^{1}$ H NMR (400 MHz, DMSO- $^{4}$ 6):  $\delta$  2.51 (s, 3H, CH<sub>3</sub>–C=N), 2.62 (s, 3H, CH<sub>3</sub>), 7.40 (s, 1H, thiazolyl-C<sub>5</sub>-H), 7.47 (d,  $^{1}$  = 8.4 Hz, 2H, 4-chlorophenyl-C<sub>3,5</sub>-H), 7.80 (d,  $^{1}$  = 8.4 Hz, 2H, 1-carboxyphenyl-C<sub>3,5</sub>-H), 7.89 (d,  $^{1}$  = 8.4 Hz, 2H, 4-chlorophenyl-C<sub>2,6</sub>-H), 8.18 (d,  $^{1}$  = 8.4 Hz, 2H, 1-carboxyphenyl-C<sub>2,6</sub>-H), 11.59 (s, 1H, NH, D<sub>2</sub>O exchangeable).  $^{13}$ C NMR (100 MHz, DMSO- $^{1}$ 6):  $\delta$  11.4, 14.9, 100.0, 105.3, 125.8, 127.7, 129.1, 131.1, 132.3, 132.4, 132.6, 134.1, 139.4, 142.9, 1432.2, 166.9, 170.1. ESI-MS  $^{1}$ 8 ( $^{1}$ 7 + 1], 451.1 [M $^{+}$  - 1]. Anal. Calcd for C<sub>21</sub>H<sub>17</sub>ClN<sub>6</sub>O<sub>2</sub>S (452.92) C, 55.69; H, 3.78; N, 18.56; S, 7.08. Found: C, 55.88; H, 3.91; N, 18.69; S, 7.23.

4.1.6.4. 4-[4-[1-(2-(4-(4-Chlorophenyl)thiazol-2-yl)hydrazineylidene)ethyl]-5-methyl-1H-1,2,3-triazol-1-yl]benzenesulfonamide (5d). Brick red powder; yield 67%, m.p. 209–211 °C. IR (KBr, cm<sup>-1</sup>): 3465 (NH), 3346, 3265 (NH<sub>2</sub>), 1635 (C=N), 1557 (C=C), 1274, 1104 (S= O), 688 (C-S-C). <sup>1</sup>H NMR (400 MHz, DMSO- $d_6$ ):  $\delta$  2.51 (s, 3H, CH<sub>3</sub>-C=N), 2.63 (s, 3H, CH<sub>3</sub>), 7.42 (s, 1H, thiazolyl-C<sub>5</sub>-H), 7.48 (d, J = 8.4 Hz, 2H, 4-chlorophenyl-C<sub>3,5</sub>-H), 7.60 (s, 2H, SO<sub>2</sub>NH<sub>2</sub>, D<sub>2</sub>O exchangeable), 7.83 (d, J = 8.4 Hz, 2H, 1-sulfamoylphenyl- $C_{2.6}$ -H), 7.90 (d, J = 8.4 Hz, 2H, 4-chlorophenyl- $C_{2,6}$ -H), 8.08 (d, J = 8.4 Hz, 2H, 1-sulfamoylphenyl-C<sub>3.5</sub>-H), 11.54 (s, 1H, NH, D<sub>2</sub>O exchangeable).  $^{13}\text{C NMR}$  (100 MHz, DMSO- $d_6$ ):  $\delta$  11.4, 14.9, 105.2, 126.4, 126.4, 127.7, 127.8, 129.1, 132.8, 133.6, 138.3, 138.5, 143.0, 145.5, 145.5, 170.1. HRMS-ESI: Calcd for  $C_{20}H_{18}CIN_7O_2S_2Na$   $[M+Na]^+$  510.054413, Found: 510.054412. Anal. Calcd for C<sub>20</sub>H<sub>18</sub>ClN<sub>7</sub>O<sub>2</sub>S<sub>2</sub> (487.99) C, 49.23; H, 3.72; N, 20.09; S, 13.14. Found: C, 49.54; H, 3.84; N, 19.87; S, 13.38.

4.1.6.5. 4-[4-[1-(2-(4-(4-Chlorophenyl)thiazol-2-yl)hydrazineylidene)ethyl]-5-methyl-1H-1,2,3-triazol-1-yl]-N-(thiazol-2-yl)benzenesulfonamide (5e). Buff powder; yield 67%, m.p. 188-190 °C. IR (KBr, cm<sup>-1</sup>): 3445 (NH), 1640 (C=N), 1530 (C=C), 1290, 1141 (S= O), 693 (C-S-C). <sup>1</sup>H NMR (400 MHz, DMSO- $d_6$ ):  $\delta$  2.51 (s, 3H,  $CH_3-C=N$ ), 2.61 (s, 3H,  $CH_3$ ), 6.90 (d, J=4.8 Hz, 1H, 2sulfamoylthiazolyl- $C_5$ -H), 7.31 (d, J = 4.8 Hz, 1H, 2sulfamoylthiazolyl- $C_4$ -H), 7.41 (s, 1H, thiazolyl- $C_5$ -H), 7.48 (d, J = 8.4 Hz, 2H, 4-chlorophenyl-C<sub>3, 5</sub>-H), 7.84–7.91 (m, 4H, 1-4-chlorophenyl-C<sub>2,6</sub>-H), sulfamoylphenyl-C<sub>2,6</sub>-H, J = 8.4 Hz, 2H, 1-sulfamoylphenyl-C<sub>3,5</sub>-H), 11.44 (s, 1H, NH, D<sub>2</sub>O exchangeable), 12.96 (s, 1H, SO<sub>2</sub>NH, D<sub>2</sub>O exchangeable). <sup>13</sup>C NMR (100 MHz, DMSO- $d_6$ ):  $\delta$  11.4, 14.9, 105.3, 109.2, 125.2, 126.3, 127.7, 127.8, 129.1, 132.4, 132.7, 134.1, 134.1, 142.9, 143.8, 149.5, 169.7, 170.1. EI-MS m/z: 572.59 [M<sup>+</sup>·+2], 571.97 [M<sup>+</sup>·+1]. Anal. Calcd for C<sub>23</sub>H<sub>19</sub>ClN<sub>8</sub>O<sub>2</sub>S<sub>3</sub> (571.1) C, 48.37; H, 3.35; N, 19.62; S, 16.84. Found: C, 48.51; H, 3.47; N, 19.79; S, 17.01.

### 4.1.7. General procedure for the synthesis of compounds **6a-e**

A mixture of the appropriate ketone (**2a-e**) (5 mmol), phenyl hydrazine (0.54 g, 0.49 ml, 5 mmol) and few drops of glacial acetic acid was refluxed in ethanol (20 ml) for 12–16 h, left to cool. The formed precipitate was filtered, dried and used for next step without purification.

4.1.7.1. 1 - (4 - Fl u o r o p h e n y l) - 5 - m e t h y l - 4 - [1 - (2 - phenylhydrazineylidene)ethyl]-1H-1,2,3-triazole (6b). Creamy powder; yield 67%, m.p. 193–195 °C. IR (KBr, cm $^{-1}$ ): 3385 (NH), 1638 (C=N), 1595 (C=C).  $^{1}$ H NMR (400 MHz, DMSO- $^{4}$ 6):  $\delta$  2.45 (s, 3H, CH<sub>3</sub>–C=N), 2.57 (s, 3H, CH<sub>3</sub>), 6.74–6.78 (m, 1H, pheny-C<sub>4</sub>-H), 7.17–7.25 (m, 4H, phenyl-C<sub>2,3,5,6</sub>-H), 7.47–7.52 (m, 2H, 4-fluorophenyl-C<sub>3,5</sub>-H), 7.69–7.73 (m, 2H, 4-fluorophenyl-C<sub>2,6</sub>-H), 9.31 (s, 1H, NH, D<sub>2</sub>O exchangeable).  $^{13}$ C NMR (100 MHz, DMSO- $^{4}$ 6):  $\delta$  11.2, 13.8, 113.0, 117.0, 119.3, 128.2, 129.4, 131.5, 132.7, 137.5, 143.8, 146.4, 161.6. ESI-MS  $^{m}$ / $^{2}$ : 310.0 [M $^{++}$ +1], 308.0 [M $^{+-}$ -1]. Anal. Calcd for C<sub>17</sub>H<sub>16</sub>FN<sub>5</sub> (309.34) C, 66.01; H, 5.21; N, 22.64. Found: C, 65.96; H, 5.34; N, 22.50.

4.1.7.2. 4-[5-Methyl-4-[1-(2-phenylhydrazineylidene)ethyl]-1H-1,2,3-triazol-1-yl]benzoic acid (**6c**). Light yellow powder; yield 67%, m.p. 234–236 °C. IR (KBr, cm<sup>-1</sup>): 3464 (OH), 3359 (NH), 1691 (C= O), 1654 (C=N), 1599 (C=C). <sup>1</sup>H NMR (400 MHz, DMSO- $d_6$ ):  $\delta$  2.45 (s, 3H, CH<sub>3</sub>–C=N), 2.65 (s, 3H, CH<sub>3</sub>), 6.75–6.78 (m, 1H, pheny-C<sub>4</sub>-H), 7.17–7.25 (m, 4H, phenyl-C<sub>2,3,5,6</sub>-H), 7.80 (d, J = 8.4 Hz, 2H, 1-carboxyphenyl-C<sub>3,5</sub>-H), 8.18 (d, J = 8.4 Hz, 2H, 1-carboxyphenyl-C<sub>2,6</sub>-H), 9.34 (s, 1H, NH, D<sub>2</sub>O exchangeable), 13.36 (s, 1H, COOH, D<sub>2</sub>O exchangeable). <sup>13</sup>C NMR (100 MHz, DMSO- $d_6$ ):  $\delta$  11.4, 13.9, 113.0, 119.3, 125.7, 129.7, 131.1, 131.3, 132.2, 137.4, 139.6, 144.2, 146.4, 166.9.

ESI-MS m/z: 334.1 [M<sup>++</sup>+1], 336.1 [M<sup>++</sup>-1]. Anal. Calcd for  $C_{18}H_{17}N_5O_2$  (335.36) C, 64.47; H, 5.11; N, 20.88. Found: C, 64.63; H, 5.28; N, 21.12.

4.1.7.3. 4-[5-Methyl-4-[1-(2-phenylhydrazineylidene)ethyl]-1H-1,2,3-triazol-1-yl]benzenesulfonamide (6d). Yellow powder; yield 67%, m.p. 265–268 °C. IR (KBr cm $^{-1}$ ): 3410 (NH), 3325, 3176 (NH<sub>2</sub>), 1628 (C=N), 1594 (C=C), 1250, 1155 (S=O). <sup>1</sup>H NMR (400 MHz, DMSO- $^{-1}$ 6):  $\delta$  2.45 (s, 3H, CH<sub>3</sub>–C=N), 2.65 (s, 3H, CH<sub>3</sub>), 6.75–6.79 (m, 1H, pheny-C<sub>4</sub>–H), 7.17–7.26 (m, 4H, phenyl-C<sub>2,3,5,6</sub>–H), 7.60 (s, 2H, SO<sub>2</sub>NH<sub>2</sub>, D<sub>2</sub>O exchangeable), 7.89 (d, J = 8.4 Hz, 2H, 1-sulfamoylphenyl-C<sub>3,5</sub>–H), 8.05 (d, J = 8.4 Hz, 2H, 1-sulfamoylphenyl-C<sub>3,5</sub>–H), 9.35 (s, 1H, NH, D<sub>2</sub>O exchangeable). <sup>13</sup>C NMR (100 MHz, DMSO- $^{-1}$ 6):  $\delta$  11.4, 13.9, 113.0, 119.4, 126.2, 127.6, 129.5, 131.4, 137.3, 138.6, 144.3, 145.3, 146.4. ESI-MS  $^{-1}$ 8 (370.43) C, 55.12; H, 4.90; N, 22.69; S, 8.66. Found: C, 55.30; H, 5.17; N, 22.86; S, 8.79.

4.1.7.4. 4-[5-Methyl-4-[1-(2-phenylhydrazineylidene)ethyl]-1H-1,2,3-triazol-1-yl]-N-(thiazol-2-yl)benzenesulfonamide (**6e**). Creamy powder; yield 67%, m.p. 250–253 °C. IR (KBr cm $^{-1}$ ): 3436, 3337 (NH), 1667 (C=N), 1589 (C=C), 1269, 1136 (S=O). <sup>1</sup>H NMR (400 MHz, DMSO- $d_6$ ):  $\delta$  2.44 (s, 3H, CH<sub>3</sub>–C=N), 2.63 (s, 3H, CH<sub>3</sub>), 6.74–6.78 (m, 1H, pheny-C<sub>4</sub>–H), 6.9 (d, J = 4.8 Hz, 1H, thiazolyl-C<sub>5</sub>–H), 7.17–7.25 (m, 4H, phenyl-C<sub>2, 3,5,6</sub>–H), 7.31 (d, J = 4.8 Hz, 1H, thiazolyl-C<sub>4</sub>–H), 7.84 (d, J = 8.4 Hz, 2H, 1-sulfamoylphenyl-C<sub>2,6</sub>–H), 8.04 (d, J = 8.4 Hz, 2H, 1-sulfamoylphenyl-C<sub>3,5</sub>–H), 9.35 (s, 1H, NH, D<sub>2</sub>O exchangeable), 12.94 (s, 1H, SO<sub>2</sub>NH, D<sub>2</sub>O exchangeable). <sup>13</sup>C NMR (100 MHz, DMSO- $d_6$ ):  $\delta$  11.4, 109.2, 113.0, 119.3, 125.1, 126.1, 127.7, 129.4, 131.4, 137.3, 138.8, 143.6, 144.3, 146.4, 169.6. ESI-MS m/z: 454.1 [M $^{++}$ +1]. Anal. Calcd for C<sub>20</sub>H<sub>19</sub>N<sub>7</sub>O<sub>2</sub>S<sub>2</sub> (453.54) C, 52.96; H, 4.22; N, 21.62; S, 14.14. Found: C, 53.20; H, 4.35; N, 21.84; S, 14.36.

### 4.1.8. General procedure for the synthesis of compounds 7a-e

To an ice-cold solution of the appropriate hydrazone derivative (**6a-e**) (3 mmol) in dimethylformamide (5 ml), phosphorous oxychloride (2 g, 1.2 ml, 13 mmol) was added dropwise. After the addition was completed, the reaction mixture was stirred for 30 min at room temperature and then stirred at 60–65 °C for 8 h. The reaction mixture was quenched into ice cold water. The solids thus precipitated were filtered, dried and crystallized from DMF/water.

4.1.8.1. 3-[1-(4-Fluorophenyl)-5-methyl-1H-1,2,3-triazol-4-yl]-1-phenyl-1H-pyrazole-4-carbaldehyde (7b). Buff powder; yield 67%, m.p. 157–159 °C. IR (KBr, cm<sup>-1</sup>): 1701 (C=O), 1668 (C=N), 1604 (C=C). ¹H NMR (400 MHz, DMSO- $d_6$ ):  $\delta$  2.64 (s, 3H, CH<sub>3</sub>), 7.42–7.45 (m, 1H, phenyl-C<sub>4</sub>-H), 7.51–7.60 (m, 4H, 4-fluorophenyl-C<sub>3,5</sub>-H and phenyl-C<sub>3,5</sub>-H), 7.78–7.81 (m, 2H, 4-fluorophenyl-C<sub>2,6</sub>-H), 8.02–8.04 (m, 2H, phenyl-C<sub>2,6</sub>-H), 9.29 (s, 1H, pyrazolyl-C<sub>5</sub>-H), 10.57 (s, 1H, CHO). ¹³C NMR (100 MHz, DMSO- $d_6$ ): 10.2, 117.1, 119.7, 123.6, 128.3, 128.4, 130.2, 131.1, 132.5, 134.0, 137.7, 139.0, 146.3, 161.7, 187.1. ESI-MS m/z: 348.1 [M<sup>+-</sup>+1]. Anal. Calcd for C<sub>19</sub>H<sub>14</sub>FN<sub>5</sub>O (347.35) C, 65.70; H, 4.06; N, 20.16. Found: C, 65.87; H, 4.24; N, 20.39.

4.1.8.2. 4-[4-(4-Formyl-1-phenyl-1H-pyrazol-3-yl)-5-methyl-1H-1,2,3-triazol-1-yl]benzoic acid (7c). Off white powder; yield 67%, m.p. 225–227 °C. IR (KBr, cm $^{-1}$ ): 3425 (OH), 1717 (C=O carbaldehyde), 1685 (C=O carboxylic acid), 1654 (C=N), 1609 (C=C).  $^{1}$ H NMR (400 MHz, DMSO- $d_6$ ):  $\delta$  2.70 (s, 3H, CH<sub>3</sub>), 7.41–7.45 (m, 1H, phenyl-C<sub>4</sub>-H), 7.55–7.59 (m, 2H, phenyl-C<sub>3,5</sub>-H), 7.86 (d, J = 8.4 Hz, 2H, 1-carboxyphenyl-C<sub>3,5</sub>-H), 8.01–8.03 (m, 2H, phenyl-C<sub>2,6</sub>-H), 8.20 (d, J = 8.4 Hz, 2H, 1-carboxyphenyl-C<sub>2,6</sub>-H), 9.31 (s, 1H,

pyrazolyl-C<sub>5</sub>-H), 10.57 (s, 1H, CHO). <sup>13</sup>C NMR (100 MHz, DMSO- $d_6$ ):  $\delta$  10.4, 119.7, 123.6, 125.7, 128.3, 130.2, 131.1, 131.2, 132.5, 133.9, 138.0, 139.0, 139.3, 146.1, 166.9, 187.1. ESI-MS m/z: 374.1 [M++1], 372.1 [M++-1]. Anal. Calcd for  $C_{20}H_{15}N_5O_3$  (373.36) C, 64.34; H, 4.05; N, 18.76. Found: C, 64.58; H, 4.18; N, 19.03.

4.1.8.3. 4-[4-(4-Formyl-1-phenyl-1H-pyrazol-3-yl)-5-methyl-1H-1,2,3-triazol-1-yl]benzenesulfonamide (7d). Buff powder; yield 67%, m.p. 209–211 °C. IR (KBr cm<sup>-1</sup>): 3358, 3256 (NH<sub>2</sub>), 1703 (C=O), 1679 (C=N), 1637 (C=C), 1282, 1149 (SO<sub>2</sub>), <sup>1</sup>H NMR (400 MHz, DMSO- $d_6$ ):  $\delta$  2.71 (s, 3H, CH<sub>3</sub>), 7.42–7.46 (m, 1H, phenyl-C<sub>4</sub>-H), 7.57–7.61 (m, 2H, phenyl-C<sub>3,5</sub>-H), 7.91 (d, J = 8.4 Hz, 2H, 1-sulfamoylphenyl-C<sub>2,6</sub>-H, 8.03–8.07 (m, 4H, phenyl-C<sub>2,6</sub>-H, 1-sylfamoylphenyl-C<sub>3,5</sub>-H), 9.31 (s, 1H, pyrazolyl-C<sub>5</sub>-H), 10.56 (s, 1H, CHO). <sup>13</sup>C NMR (100 MHz, DMSO- $d_6$ ):  $\delta$  10.4, 119.7, 123.7, 126.2, 128.0, 128.3, 130.2, 131.2, 134.1, 138.0, 138.4, 139.0, 144.6, 146.1, 187.1. EI-MS m/z: 408.32 [M<sup>+-</sup>]. Anal. Calcd for C<sub>19</sub>H<sub>16</sub>N<sub>6</sub>O<sub>3</sub>S (408.43) C, 55.87; H, 3.95; N, 20.58; S, 7.85. Found: C, 56.09; H, 4.11; N, 20.75; S, 7.92.

4.1.8.4. 4-[4-(4-Formyl-1-phenyl-1H-pyrazol-3-yl)-5-methyl-1H-1,2,3-triazol-1-yl]benzenesulfonic acid (7e). Beige powder; yield 67%, m.p. >300 °C. IR (KBr cm<sup>-1</sup>): 1703 (C=O), 1669 (C=N), 1598 (C=C), 1359, 1122 (S=O). <sup>1</sup>H NMR (400 MHz, DMSO- $d_6$ ): δ 2.68 (s, 3H, CH<sub>3</sub>), 7.42–7.46 (m, 1H, phenyl-C<sub>4</sub>-H), 7.56–7.6 (m, 2H, phenyl-C<sub>3,5</sub>-H), 7.69 (d, J=7.6 Hz, 2H, 1-sulfophenyl-C<sub>2,6</sub>-H), 7.88 (d, J=7.6 Hz, 2H, 1-sulfolphenyl-C<sub>3,5</sub>-H), 8.03–8.05 (m, 2H, phenyl-C<sub>2,6</sub>-H), 9.29 (s, 1H, pyrazolyl-C<sub>5</sub>-H), 10.58 (s, 1H, CHO). <sup>13</sup>C NMR (100 MHz, DMSO- $d_6$ ): δ 10.3, 119.7, 123.7, 125.3, 127.4, 128.3, 130.2, 131.1, 133.8, 135.9, 137.8, 139.0, 146.4, 150.0, 187.1. ESI-MS m/z: 410.1 [M<sup>++</sup>+1]. Anal. Calcd for C<sub>19</sub>H<sub>15</sub>N<sub>5</sub>O<sub>4</sub>S (409.42) C, 55.74; H, 3.69; N, 17.11; S, 7.83. Found: C, 55.98; H, 3.81; N, 17.24; S, 7.81.

### 4.1.9. General procedure for the synthesis of compounds 8a-d

A mixture of the appropriate aldehyde **7a,b,d,e** (2 mmol), hydroxylamine hydrochloride (0.17 g, 2.5 mmol) and sodium acetate (0.2 g, 2.5 mmol) in ethanol (10 ml) was refluxed for 8–12 h, then left to cool. The separated solid was then filtered, dried and crystallized from aqueous ethanol.

4.1.9.1. 3-[1-(4-Chlorophenyl)-5-methyl-1H-1,2,3-triazol-4-yl]-1-phenyl-1H-pyrazole-4-carbaldehyde oxime (8a). Beige powder; yield 65%, m.p. 197—199 °C. IR (KBr, cm $^{-1}$ ): 3488 (OH), 1645 (C=N), 1594 (C=C). <sup>1</sup>H NMR (400 MHz, DMSO- $d_6$ ):  $\delta$  2.65 (s, 3H, CH<sub>3</sub>), 7.37—7.41 (m, 1H, phenyl-C<sub>4</sub>-H), 7.54—7.58 (m, 2H, phenyl-C<sub>3,5</sub>-H), 7.73—7.79 (m, 4H, 4-chlorophenyl-H), 7.95—7.97 (m, 2H, phenyl-C<sub>2,6</sub>-H), 8.34 (s, 1H, CH=N), 9.21 (s, 1H, pyrazolyl-C<sub>5</sub>-H), 11.79 (s, 1H, N=OH, D<sub>2</sub>O exchangeable). <sup>13</sup>C NMR (100 MHz, DMSO- $d_6$ ):  $\delta$  10.4, 112.9, 119.4, 127.5, 127.6, 130.2, 130.2, 131.7, 133.5, 134.9, 135.1, 137.9, 138.4, 139.5, 144.0. ESI-MS m/z: 379.1 [M $^+$ +1]. Anal. Calcd for C<sub>19</sub>H<sub>15</sub>ClN<sub>6</sub>O (378.82) C, 60.24; H, 3.99; N, 22.19. Found: C, 60.13; H, 4.16; N, 22.41.

4.1.9.2. 3-[1-(4-Fluorophenyl)-5-methyl-1H-1,2,3-triazol-4-yl]-1-phenyl-1H-pyrazole-4-carbaldehyde oxime**(8b)** $. Beige powder; yield 58%, m.p. 182–184 °C. IR (KBr, cm<sup>-1</sup>): 3511 (OH), 1642 (C=N), 1603 (C=C). <sup>1</sup>H NMR (400 MHz, DMSO-<math>d_6$ ):  $\delta$  2.63 (s, 3H, CH<sub>3</sub>), 7.37–7.41 (m, 1H, phenyl-C<sub>4</sub>-H), 7.50–7.57 (m, 4H, 4-fluorophenyl-C<sub>3,5</sub>-H and phenyl-C<sub>3,5</sub>-H), 7.77–7.81 (m, 2H, 4-fluorophenyl-C<sub>2,6</sub>-H), 7.95–7.97 (m, 2H, phenyl-C<sub>2,6</sub>-H), 8.35 (s, 1H, CH=N), 9.21 (s, 1H, pyrazolyl-C<sub>5</sub>-H), 11.79 (s, 1H, N-OH, D<sub>2</sub>O exchangeable. <sup>13</sup>C (100 MHz, DMSO- $d_6$ ):  $\delta$  10.2, 112.9, 117.0, 119.4, 127.5, 128.3, 130.2131.7, 132.6, 133.6, 137.9, 139.5, 144.0, 161.7. ESI-MS m/z: 363.1 [M<sup>+</sup>+1], 361.1 [M<sup>+</sup>-1]. Anal. Calcd for C<sub>19</sub>H<sub>15</sub>FN<sub>6</sub>O (362.36) C, 62.98; H, 4.17; N, 23.19. Found: C, 63.24; H, 4.23; N, 23.45.

4.1.9.3. 4-[4-[4-((Hydroxyimino)methyl)-1-phenyl-1H-pyrazol-3-yl]-5-methyl-1H-1,2,3-triazol-1-yl]benzenesulfonamide (8c). Beige powder; yield 64%, m.p. 241–243 °C. IR (KBr, cm $^{-1}$ ): 3512 (OH), 3358, 3230 (NH<sub>2</sub>), 1644 (C=N), 1602 (C=C), 1286, 1150 (S=O).  $^{1}$ H NMR (400 MHz, DMSO- $d_6$ ):  $\delta$  2.69 (s, 3H, CH<sub>3</sub>), 7.36–7.42 (m, 1H, phenyl-C<sub>4</sub>-H), 7.53–7.57 (m, 2H, phenyl-C<sub>3,5</sub>-H), 7.89–8.06 (m, 6H, 1-sulfamoylphenyl-H and phenyl-C<sub>3,5</sub>-H), 8.31 (s, 1H, CH=N), 9.21 (s, 1H, pyrazolyl-C<sub>5</sub>-H).  $^{13}$ C NMR (100 MHz, DMSO- $d_6$ ):  $\delta$  10.4, 113.0, 119.4, 126.1, 126.2, 127.9, 130.1, 130.2, 131.7, 133.1, 138.5, 138.7, 139.5, 139.5, 143.9, 144.5. EI-MS m/z: 423.33 [M $^{+-}$ ]. Anal. Calcd for C<sub>19</sub>H<sub>17</sub>N<sub>7</sub>O<sub>3</sub>S (423.45) C, 53.89; H, 4.05; N, 23.15; S, 7.57. Found: C, 54.16; H, 4.31; N, 23.42; S, 7.70.

4.1.9.4. 4-[4-[4-((Hydroxyimino)methyl)-1-phenyl-1H-pyrazol-3-yl]-5-methyl-1H-1,2,3-triazol-1-yl]benzenesulfonic acid (**8d**). Off white powder; yield 56%; m.p. 250–252 °C. IR (KBr, cm<sup>-1</sup>): 3508 (OH), 3436 (NH), 1645 (C=N), 1597 (C=C), 1322, 1165 (S=O).  $^{1}$ H NMR (400 MHz, DMSO- $d_6$ ):  $\delta$  2.65 (s, 3H, CH<sub>3</sub>), 7.37–7.41 (m, 1H, phenyl-C<sub>4</sub>-H), 7.54–7.57 (m, 2H, phenyl-C<sub>3,5</sub>-H), 7.68 (d, J=7.6 Hz, 2H, 1-sulfophenyl-C<sub>2,6</sub>-H), 7.87 (d, J=7.6 Hz, 2H, 1-sulfophenyl-C<sub>3,5</sub>-H), 7.96–7.98 (m, 2H, phenyl-C<sub>2,6</sub>-H), 8.34 (s, 1H, CH=N), 9.20 (s, 1H, pyrazolyl-C<sub>5</sub>-H).  $^{13}$ C NMR (100 MHz, DMSO- $d_6$ ):  $\delta$  10.4, 112.9, 119.4, 125.3, 127.3, 127.5, 130.2, 131.7, 133.4, 136.1, 137.9, 138.4, 139.5, 144.1, 149.9. ESI-MS m/z: 425.1 [M++1]. Anal. Calcd for C<sub>19</sub>H<sub>16</sub>N<sub>6</sub>O<sub>4</sub>S (424.43) C, 53.77; H, 3.80; N, 19.80; S, 7.55. Found: C, 54.03; H, 3.94; N, 19.64; S, 7.63.

#### 4.2. Biological evaluation

### 4.2.1. In vitro COX-1, COX-2 and 15-LOX inhibitory activities

Cayman colorimetric COX (ovine) inhibitor screening assay kit (Catalog No. 560131) supplied by Cayman chemicals, Ann Arbor, MI, USA, was used to screen all the synthesized target compounds for their COX-1 and COX-2 inhibitory activities. Similarly, Cayman lipoxygenase inhibitor screening assay kit Catalog No. (760,700) supplied by Cayman chemicals, Ann Arbor, MI, USA, was used to screen for the ability of the same compounds to inhibit soya bean 15-LOX.All test solutions and reagents as well as experimental procedures were carried out in agreement with both the manufacturer's instructions and our previously reported studies [22,23].

### 4.2.2. Carbonic anhydrase inhibition

Applied Photophysics stopped-flow instrument was used to measure the CA catalysed CO<sub>2</sub> hydration activities of the selected compounds (**2d-e**, **3d-e**, **4b-e**, **5a**,**c-e** and **8a-d**), as described earlier [40].

### 4.2.3. In vitro anti-proliferative activity

MCF-7: Breast Adenocarcinoma cell line, A549: Lung cancer cell line, HepG2: Hepatocellular carcinoma and WI-38: Normal Human Lung Fibroblasts cell lines were obtained from Nawah Scientific Inc., (Mokatam, Cairo, Egypt). Cells were maintained in DMEM media supplemented with 100 mg/mL of streptomycin, 100 units/mL of penicillin and 10% of heat-inactivated fetal bovine serum (FBS) in humidified, 5% (v/v) CO<sub>2</sub> atmosphere at 37 °C. Cell viability was assessed by SRB assay according to previously reported studies [41,42]. In brief, aliquots of 100  $\mu$ L cell suspension (5  $\times$  10<sup>3</sup> cells) were in 96-well plates and incubated in complete media for 24h. Cells were treated with another aliquot of 100 µL media containing test compounds at various concentrations (0.01, 0.1,1,10,100 μM). After 72 h of drug exposure, cells were fixed by replacing media with 150 μL of 10% TCA (Trichloro acetic acid) and incubated at 4 °C for 1 h. After the removal of TCA solution followed by appropriate washing with distilled water, aliquots of 70 μL SRB (Sulforhodamine B) solution (0.4% w/v) were added and incubated in a dark place at room temperature for 10 min. Plates were washed 3 times with 1% acetic acid and allowed to air-dry overnight. Then, 150  $\mu L$  of 10 mM Tris—base was added to dissolve protein-bound SRB stain; the absorbance was measured at 540 nm using a BMG LABTECH®-FLUOstar Omega microplate reader (Ortenberg, Germany). Doseresponse curves were plotted for each compound using SigmaPlot software and  $\rm IC_{50}$  values were determined and reported as the average from three replicates  $\pm$  SD.

### 4.2.4. Inhibition of 6-keto-PGF1 $\alpha$ expression cell-based assay

**Cell culture:** THP-1 Cell culture and differentiation were conducted as previously described [69]. Briefly, THP-1 cells (human acute monocytic leukaemia lineage, American Type Culture Collection, Manassas, VA) were cultured in RPMI-1640 (Lonza, Basel, Switzerland) containing 10% fetal bovine serum (FBS), glucose (11 mmol/L), L-glutamine (4 mmol/L), pyruvate (1 mM), penicillin (100 U/mL), and streptomycin (100 mg/mL) and incubated at 37 °C in a humidified atmosphere of 5% CO2 and 95% air. Furthermore, HT-29 cells human colorectal adenocarcinoma cells were cultured in High glucose Dulbecco's Modified Eagle's medium (DMEM) supplemented with 10% FBS and 1% penicillin/streptomycin, and incubated in a humidified incubator at 37 °C with 5% CO2 atmosphere and 95% air.

Cytotoxicity assay: In order to select the concentration of compounds, a cytotoxicity assay was conducted. THP-1 cells were seeded in a 96-well plate at a density of 20,000 cells/well. After challenging of THP-1 cells with 25 nM PMA for 24 h and 100 ng/ml lipopolysaccharide (LPS, invivogen, San Diego, CA, USA) for 24 h, the differentiated macrophages were treated with different drug concentrations for 24 h. HT-29 cells were seeded in a 96-well plate at a seeding density of 10,000 cells/well. Following adhesion, HT-29 cells were then treated with different drug concentrations for 24 h. Untreated cells were used as a negative control. Diclofenac was used as a positive control. Cell viability was evaluated using MTS colorimetric cell viability kit (Abcam, Cambridge, UK). Cell viability experiments were conducted in triplicates from three different cell batches. Best fit IC<sub>50</sub> values were determined by nonlinear regression using GraphPad Prism 8 Software (GraphPad, San Diego, CA).

6-keto-Prostaglandin F1 alpha levels: THP-1 cells were seeded in a 12-well plate at a density of 300,000 cells/well. THP-1 monocytes were differentiated into macrophages by incubation with 25 nM of phorbol myristate-acetate (PMA, Calbiochem, Darmstadt, Germany) for 24 h, followed by LPS 100 ng/ml for 3 h. THP-1 cells were then treated with compounds **5a** (300  $\mu$ M) and **5d** (300  $\mu$ M) for 48 h. HT-29 cells were seeded in a 12-well plate at a density of 250,000 cells/well and treated with 1 µg/ml LPS [14]. Following adhesion, cells were treated with compounds 5a (100 µM) and 5d (100  $\mu$ M) for 48 h. Diclofenac (300  $\mu$ M) was used as a positive control. Afterwards, supernatants were centrifugated at 14,000 rpm for 10 min at 4 °C. 6-keto-Prostaglandin F1 alpha (6keto-PGF1α) production was evaluated using the 6-keto-PGF1α Enzyme linked immunosorbent assay (ELISA) kit (Abcam, Cambridge, UK) according to the manufacturer's protocol. In view of the cytotoxic nature of the compounds, the obtained values were compared to that of the known COX-inhibitor diclofenac, whose selected concentration (300 µM) demonstrated comparable cell viability levels. 6-keto-PGF1α concentration was measured in triplicates from three different cell batches.

### 4.2.5. Flow cytometric cell cycle analysis

As described earlier [70], MCF-7 and A549 cells were seeded into six-well plates at a density of 2  $\times$  10<sup>5</sup> cells per well and incubated for 24 h. The cells were cultured in RPMI 1640 supplemented with fetal bovine serum (FBS, 10%) and incubated at 37 °C

and 5% CO<sub>2</sub>. The medium was removed and replaced with media (final DMSO concentration, 1% v/v) containing compounds **5a** and **5d** (used at their corresponding  $\mu$ M IC<sub>50</sub>). After incubation for 24 h the cell layer was trypsinized and washed with cold PBS and fixed with 70% ethanol. The fixed cells were rinsed with PBS and then stained with the DNA fluorochrome PI in a solution containing Triton X-100 as well as RNase, and kept for 15 min at 37 °C, according the instruction's manual. Then the samples were analyzed with a FACS Caliber flow cytometer (Becton Dickinson & Co., Franklin Lakes, NJ). The number of cells analyzed for each sample was 10,000.

### 4.2.6. Annexin V-FITC/propidium iodide analysis of apoptosis

Staining and counterstaining of MCF-7 cells were performed with Annexin V- fluorescein isothiocyanate (FITC) and propidium iodide (PI), respectively, using Annexin V-FITC/PI apoptosis detection kit and as described earlier [70].  $2 \times 10^5$  Cells were exposed to compound **5a** and **5d** (used at their corresponding  $\mu$ M IC<sub>50</sub>) for 24 h. After trypsinization, appropriate washing with PBS and staining with FITC and PI (5  $\mu$ L each in binding buffer for 15 min at 37 °C in the dark), samples were analyzed with FACS Caliber flow cytometer (Becton Dickinson Biosciences & Co., Franklin Lakes, NJ). The number of cells analyzed for each sample was 10,000.

### 4.2.7. Effect on the expression levels of Bcl-2, Bax and caspase-9

After growing the MCF-7 and A549 cells in RPMI 1640 containing 10% fetal bovine serum at 37 °C, they were treated with compounds **5a** and **5d** (used at their corresponding μM IC<sub>50</sub>) respectively, and lysed with cell Extraction Buffer. This lysate was diluted in Standard Diluent Buffer over the range of the assay and measured for human active Bax, Bcl-2 and caspase-9 content using DRG Human Bax ELISA Kit (EIA-4487), DRG®, USA and Zymed Bcl-2 ELISA Kit (99–0042), Zymed® Laboratories, Invitrogen Immunodetection, Canada, and DRG Caspase-9(human) ELISA (EIA-4860) DRG®, USA respectively, following manufacturer's instructions for each kit.

### 4.2.8. In vivo antitumor activity in MCF-7 xenograft model

**LD**<sub>50</sub> **calculation:** Six serial concentrations of both test and reference compounds (**8c** and 5-FU) were prepared starting with 10 mg/kg up to 60 mg/kg. Each concentration was injected intraperitoneally to a group of 10 newborn BALB/c mice of both sexes and demonstrated after 24 h and followed for 3 days. Then, LD<sub>50</sub> values were calculated [50].

Mature BALB/c mice, bred in a specific pathogen-free environment, given access to food and water ad libitum, were purchased from VACSERA R&D animal house (Egypt). Mice were housed in 12 h dark/light cycle under controlled conditions and fasted overnight. For immunosuppression, cyclosporin A (CsA, Abcam) dissolved in ethanol at a concentration of 500 mg/mL was used. An intraperitoneal injection containing 2.5 mg of CsA in emulsion of 15% v/v ethanol/castor oil, was given to the mice daily for four days before MCF-7 cell injection [51]. About 1 million MCF-7 cells in 100 μl of DMEM were injected subcutaneously in abdominal fats of each animal (26–38 g) to establish the xenograft model [52]. When the tumor mass was palpable, with a volume of around 1 cm<sup>3</sup>, the tumor-bearing mice were randomly divided into three groups; the control (vehicle-treated) group (3 mice), compound 8c-treated group (10 mice) and 5-FU treated group (10 mice). Drugs were administered by intraperitoneal injection [14] at a dose of 23 mg/kg thrice a week, for 28 days. After the start of dosing, mice were weighed every seven days and tumor volume was estimated by measuring with a Vernier caliper and calculated by the formula (tumor volume = (length  $\times$  width<sup>2</sup>)/2) [71]. As a gross indicator of toxicity, body weights were tracked throughout the study [72]. After drug treatment, all mice were euthanized as per the adopted Animal welfare and experimental procedures and in accordance with the "Guide for the Care and Use of Laboratory Animals published by US National Institute of Health (NIH publication No. 83–23, revised 1996)" and the related ethical regulations of VAC-SERA (IACUC protocol number 00202), Alexandria and Damanhour Universities.

#### 4.3. Molecular modeling

Computer-guided docking experiments were carried out using Molecular Operating Environment (MOE 2016.0802) software, Chemical Computing Group, Montreal, Canada. X-ray crystal coordinates of COX-2 (PDB code 1CX2, in complex with S58) and 15-LOX enzymes (PDB code 1LOX, in complex with RS7) were downloaded from Protein Date Bank. As well, crystal structures for human carbonic anhydrases II and XII ((hCA II-A6N complex, PDB code **5LJT**) and (hCA XII-AZM complex, PDB code **1JD0**)) were used. The active compounds, in their *E*-configuration, were prepared by hydrogens addition, partial charges calculation and energy minimization using Force Field MMFF94x. In addition, preparation of proteins was performed by omitting the repeating chains, water molecules and surfactants. MOE QuickPrep functionality was used for correcting structural issues, 3D protonation and calculation of partial charges. The default procedure in the MOE Dock protocol was utilized to detect the profitable binding poses of the studied ligands, using triangle matcher as placement method and London dG as the primary scoring function. An extra refinement step was set to rigid receptor method with GBVI/WSA dG scoring function in order to retain poses with the highest hydrophobic, ionic, and hydrogen-bond interactions with the protein. The output database comprised the scores of ligand-enzyme complexes in kcal/mol. Then, the resulting docking poses were visually examined and interactions with binding pocket residues were studied. Poses fitting into the binding pocket with the top scores and showing good ligand enzyme contacts were selected.

4.4. In silico prediction of physicochemical properties, drug likeness, pharmacokinetic profile and ligand efficiency metrics

Prediction of physicochemical properties was performed using FAF-drugs4 server, pharmacokinetic parameters by PreADMET calculator and Ligand efficiency metrics and drug likeness by Data warrior software.

### **Declaration of competing interest**

The authors declare that they have no known competing financial interests or personal relationships that could have appeared to influence the work reported in this paper.

### Appendix A. Supplementary data

Supplementary data to this article can be found online at https://doi.org/10.1016/j.ejmech.2020.112439.

### References

- [1] B. Negi, D. Kumar, W. Kumbukgolla, S. Jayaweera, P. Ponnan, R. Singh, S. Agarwal, D.S. Rawat, Anti-methicillin resistant Staphylococcus aureus activity, synergism with oxacillin and molecular docking studies of metronidazole-triazole hybrids, Eur. J. Med. Chem. 115 (2016) 426–437, https://doi.org/10.1016/j.EJMECH.2016.03.041.
- [2] E.R. Greene, S. Huang, C.N. Serhan, D. Panigrahy, Regulation of inflammation in cancer by eicosanoids, Prostag. Other Lipid Mediat. 96 (2011) 27–36, https:// doi.org/10.1016/J.PROSTAGLANDINS.2011.08.004.
- [3] A. Mantovani, Inflammation by remote control, Nature 435 (2005) 752-753,

- https://doi.org/10.1038/435752a.
- [4] R. Gomes, S. Costa, A. Colquhoun, Eicosanoids and cancer, Clinics 73 (2018) 1–10, https://doi.org/10.6061/clinics/2018/e530s.
- [5] P. Rajendran, Y.-F. Chen, Y.-F. Chen, L.-C. Chung, S. Tamilselvi, C.-Y. Shen, C.H. Day, R.-J. Chen, V.P. Viswanadha, W.-W. Kuo, C.-Y. Huang, The multifaceted link between inflammation and human diseases, J. Cell. Physiol. 233 (2018) 6458–6471, https://doi.org/10.1002/jcp.26479.
- [6] S. Agarwal, G.V. Reddy, P. Reddanna, Eicosanoids in inflammation and cancer: the role of COX-2, Expet Rev. Clin. Immunol. 5 (2009) 145–165, https://doi.org/10.1586/1744666X.5.2.145.
- [7] C. Schneider, A. Pozzi, Cyclooxygenases and lipoxygenases in cancer, Canc. Metastasis Rev. 30 (2011) 277–294, https://doi.org/10.1007/s10555-011-9310-3
- [8] L. Milas, K. Kishi, N. Hunter, K. Mason, J.L. Masferrer, P.J. Tofilon, Enhancement of tumor response to gamma-radiation by an inhibitor of cyclooxygenase-2 enzyme, J. Natl. Cancer Inst. 91 (1999) 1501–1504, https://doi.org/10.1093/ inci/91.17.1501.
- [9] O.C. Trifan, W.F. Durham, V.S. Salazar, J. Horton, B.D. Levine, B.S. Zweifel, T.W. Davis, J.L. Masferrer, Cyclooxygenase-2 inhibition with celecoxib enhances antitumor efficacy and reduces diarrhea side effect of CPT-11, Canc. Res. 62 (2002) 5778–5784.
- [10] C. Guo, D. Nie, Are lipoxygenases valid targets of cancer prevention and treatment? J. Carcinog. Mutagen. s1 (2012) 1–8, https://doi.org/10.4172/ 2157-2518.51-008.
- [11] H. Sadeghian, A. Jabbari, 15-Lipoxygenase inhibitors: a patent review, Expert Opin. Ther. Pat. 26 (2016) 65–88, https://doi.org/10.1517/ 13543776.2016.1113259.
- [12] N.K. Narayanan, D. Nargi, M. Attur, S.B. Abramson, B.A. Narayanan, Anticancer effects of licofelone (ML-3000) in prostate cancer cells, Anticancer Res. 27 (2007) 2393–2402. http://www.ncbi.nlm.nih.gov/pubmed/17695530. (Accessed 9 July 2019).
- [13] S. Kabadere, G. Kus, R. Uyar, P. Oztopcu-Vatan, Licofelone abolishes survival of carcinogenic fibroblasts by inducing apoptosis, Drug Chem. Toxicol. 37 (2014) 1–7, https://doi.org/10.3109/01480545.2013.806525.
- [14] Z. Li, Z.-C. Wang, X. Li, M. Abbas, S.-Y. Wu, S.-Z. Ren, Q.-X. Liu, Y. Liu, P.-W. Chen, Y.-T. Duan, P.-C. Lv, H.-L. Zhu, Design, synthesis and evaluation of novel diaryl-1,5-diazoles derivatives bearing morpholine as potent dual COX-2/5-LOX inhibitors and antitumor agents, Eur. J. Med. Chem. 169 (2019) 168–184, https://doi.org/10.1016/j.ejmech.2019.03.008.
- [15] H. Cai, X. Huang, S. Xu, H. Shen, P. Zhang, Y. Huang, J. Jiang, Y. Sun, B. Jiang, X. Wu, H. Yao, J. Xu, Discovery of novel hybrids of diaryl-1,2,4-triazoles and caffeic acid as dual inhibitors of cyclooxygenase-2 and 5-lipoxygenase for cancer therapy, Eur. J. Med. Chem. 108 (2016) 89–103, https://doi.org/10.1016/J.EJMECH.2015.11.013.
- [16] S. Fiorucci, R. Meli, M. Bucci, G. Cirino, Dual inhibitors of cyclooxygenase and 5-lipoxygenase. A new avenue in anti-inflammatory therapy? 1 1Abbreviations: NSAIDs, nonsteroidal anti-inflammatory drugs; COX, cyclooxygenase; LT, leukotriene; 5-LOX, 5-lipoxygenase; PG, prostaglandin; DFU, 5,5-dimet, Biochem. Pharmacol. 62 (2001) 1433–1438, https://doi.org/10.1016/S0006-2952(01)00747-X.
- [17] R. Meleddu, S. Distinto, F. Cottiglia, R. Angius, M. Gaspari, D. Taverna, C. Melis, A. Angeli, G. Bianco, S. Deplano, B. Fois, S. Del Prete, C. Capasso, S. Alcaro, F. Ortuso, M. Yanez, C.T. Supuran, E. Maccioni, Tuning the dual inhibition of carbonic anhydrase and cyclooxygenase by dihydrothiazole benzensulfonamides, ACS Med. Chem. Lett. 9 (2018) 1045–1050, https://doi.org/10.1021/acsmedchemlett.8b00352.
- [18] L. Vats, V. Sharma, A. Angeli, R. Kumar, C.T. Supuran, P.K. Sharma, Synthesis of novel 4-functionalized 1,5-diaryl-1,2,3-triazoles containing benzenesulfonamide moiety as carbonic anhydrase I, II, IV and IX inhibitors, Eur. J. Med. Chem. 150 (2018) 678–686, https://doi.org/10.1016/J.EJMECH.2018.03.030.
- [19] A.A.-M. Abdel-Aziz, A. Angeli, A.S. El-Azab, M.E.A. Hammouda, M.A. El-Sherbeny, C.T. Supuran, Synthesis and anti-inflammatory activity of sulfonamides and carboxylates incorporating trimellitimides: dual cyclooxygenase/carbonic anhydrase inhibitory actions, Bioorg. Chem. 84 (2019) 260–268, https://doi.org/10.1016/J.BIOORG.2018.11.033.
- [20] J.F. Knudsen, U. Carlsson, P. Hammarström, G.H. Sokol, L.R. Cantilena, The cyclooxygenase-2 inhibitor celecoxib is a potent inhibitor of human carbonic anhydrase II, Inflammation 28 (2004) 285–290, https://doi.org/10.1007/ s10753-004-6052-1.
- [21] G. Moussa, R. Alaaeddine, L.M. Alaeddine, R. Nassra, A.S.F. Belal, A. Ismail, A.F. El-Yazbi, Y.S. Abdel-Ghany, A. Hazzaa, Novel click modifiable thioquinazolinones as anti-inflammatory agents: design, synthesis, biological evaluation and docking study, Eur. J. Med. Chem. 144 (2018) 635–650, https://doi.org/10.1016/j.ejmech.2017.12.065.
- [22] E.D. AlFadly, P.A. Elzahhar, A. Tramarin, S. Elkazaz, H. Shaltout, M.M. Abu-Serie, J. Janockova, O. Soukup, D.A. Ghareeb, A.F. El-Yazbi, R.W. Rafeh, N.-M.Z. Bakkar, F. Kobeissy, I. Iriepa, I. Moraleda, M.N.S. Saudi, M. Bartolini, A.S.F. Belal, Tackling neuroinflammation and cholinergic deficit in Alzheimer's disease: multi-target inhibitors of cholinesterases, cyclooxygenase-2 and 15-lipoxygenase, Eur. J. Med. Chem. 167 (2019) 161–186, https://doi.org/10.1016/j.ejmech.2019.02.012.
- [23] P.A. Elzahhar, R. Alaaeddine, T.M. Ibrahim, R. Nassra, A. Ismail, B.S.K. Chua, R.L. Frkic, J.B. Bruning, N. Wallner, T. Knape, A. von Knethen, H. Labib, A.F. El-Yazbi, A.S.F. Belal, Shooting three inflammatory targets with a single bullet: novel multi-targeting anti-inflammatory glitazones, Eur. J. Med. Chem. 167

- (2019) 562-582, https://doi.org/10.1016/j.ejmech.2019.02.034.
- [24] J. Mareddy, N. Suresh, C.G. Kumar, R. Kapavarapu, A. Jayasree, S. Pal, 1,2,3-Triazole-nimesulide hybrid: their design, synthesis and evaluation as potential anticancer agents, Bioorg. Med. Chem. Lett 27 (2017) 518–523, https://doi.org/10.1016/J.BMCL.2016.12.030.
- [25] L.R.P. de Siqueira, P.A.T. de Moraes Gomes, L.P. de Lima Ferreira, M.J.B. de Melo Régo, A.C.L Leite, Multi-target compounds acting in cancer progression: focus on thiosemicarbazone, thiazole and thiazolidinone analogues, Eur. J. Med. Chem. 170 (2019) 237–260, https://doi.org/10.1016/J.EJMECH.2019.03.024.
- [26] A.H. Abdelazeem, M.T. El-Saadi, E.G. Said, B.G.M. Youssif, H.A. Omar, S.M. El-Moghazy, Novel diphenylthiazole derivatives with multi-target mechanism: synthesis, docking study, anticancer and anti-inflammatory activities, Bioorg. Chem. 75 (2017) 127–138, https://doi.org/10.1016/J.BIOORG.2017.09.009.
- [27] M. Bozdag, F. Carta, A. Angeli, S.M. Osman, F.A.S. Alasmary, Z. AlOthman, C.T. Supuran, Synthesis of N'-phenyl-N-hydroxyureas and investigation of their inhibitory activities on human carbonic anhydrases, Bioorg. Chem. 78 (2018) 1–6, https://doi.org/10.1016/j.bioorg.2018.02.029.
- [28] R.R. Ramsay, M.R. Popovic-Nikolic, K. Nikolic, E. Uliassi, M.L. Bolognesi, A perspective on multi-target drug discovery and design for complex diseases, Clin. Transl. Med. 7 (2018) 3, https://doi.org/10.1186/s40169-017-0181-2.
- [29] E. Proschak, H. Stark, D. Merk, Polypharmacology by design: a medicinal chemist's perspective on multitargeting compounds, J. Med. Chem. 62 (2019) 420–444, https://doi.org/10.1021/acs.jmedchem.8b00760.
- [30] V. Tupá, S. Drahošová, M. Grendár, M. Adamkov, Expression and association of carbonic anhydrase IX and cyclooxygenase-2 in colorectal cancer, Pathol. Res. Pract. 215 (2019) 705—711, https://doi.org/10.1016/j.prp.2019.01.012.
- [31] P. Sansone, G. Piazzi, P. Paterini, A. Strillacci, C. Ceccarelli, F. Minni, G. Biasco, P. Chieco, M. Bonafe, Cyclooxygenase-2/carbonic anhydrase-IX up-regulation promotes invasive potential and hypoxia survival in colorectal cancer cells, J. Cell Mol. Med. 13 (2009) 3876–3887, https://doi.org/10.1111/j.1582-4934.2008.00580.x.
- [32] D. González-Calderón, A. Fuentes-Benítes, E. Díaz-Torres, C.A. González-González, C. González-Romero, Azide-enolate 1,3-dipolar cycloaddition as an efficient approach for the synthesis of 1,5-disubstituted 1,2,3-triazoles from alkyl/aryl azides and β-ketophosphonates, Eur. J. Org Chem. 2016 (2016) 668–672, https://doi.org/10.1002/ejoc.201501465.
- [33] H.R.M. Rashdan, S.M. Gomha, M.S. El-Gendey, M.A. El-Hashash, A.M.M. Soliman, Eco-friendly one-pot synthesis of some new pyrazolo[1,2-b] phthalazinediones with antiproliferative efficacy on human hepatic cancer cell lines, Green Chem. Lett. Rev. 11 (2018) 264–274, https://doi.org/10.1080/ 17518253.2018.1474270.
- [34] E. Lukevics, D. Jansone, K. Rubina, E. Abele, S. Germane, L. Leite, M. Shymanska, J. Popelis, Neurotropic activity of aldehyde and ketone thiosemicarbazones with a heterocyclic component, Eur. J. Med. Chem. 30 (1995) 983–988, https://doi.org/10.1016/0223-5234(96)88318-8.
- [35] C.I. Lino, I. Gonçalves de Souza, B.M. Borelli, T.T. Silvério Matos, I.N. Santos Teixeira, J.P. Ramos, E. Maria de Souza Fagundes, P. de Oliveira Fernandes, V.G. Maltarollo, S. Johann, R.B. de Oliveira, Synthesis, molecular modeling studies and evaluation of antifungal activity of a novel series of thiazole derivatives, Eur. J. Med. Chem. 151 (2018) 248–260, https://doi.org/10.1016/ J.EJMECH.2018.03.083.
- [36] J. Easmon, G. Heinisch, J. Hofmann, T. Langer, H. Grunicke, J. Fink, G. Pürstinger, Thiazolyl and benzothiazolyl hydrazones derived from α-(N)-acetylpyridines and diazines: synthesis, antiproliferative activity and CoMFA studies, Eur. J. Med. Chem. 32 (1997) 397–408, https://doi.org/10.1016/S0223-5234(97)81677-7.
- [37] F. Minutolo, S. Bertini, C. Papi, K.E. Carlson, J.A. Katzenellenbogen, M. Macchia, Salicylaldoxime moiety as a phenolic "A-ring" substitute in estrogen receptor ligands, J. Med. Chem. 44 (2001) 4288–4291, https://doi.org/10.1021/ jm0109481.
- [38] L. Piemontese, G. Fracchiolla, A. Carrieri, M. Parente, A. Laghezza, G. Carbonara, S. Sblano, M. Tauro, F. Gilardi, P. Tortorella, A. Lavecchia, M. Crestani, B. Desvergne, F. Loiodice, Design, synthesis and biological evaluation of a class of bioisosteric oximes of the novel dual peroxisome proliferator-activated receptor α/γ ligand LT175, Eur. J. Med. Chem. 90 (2015) 583–594, https://doi.org/10.1016/J.EJMECH.2014.11.044.
- [39] C. Patrono, Cardiovascular effects of nonsteroidal anti-inflammatory drugs, Curr. Cardiol. Rep. 18 (2016) 25, https://doi.org/10.1007/s11886-016-0702-4.
- [40] R.G. Khalifah, The carbon dioxide hydration activity of carbonic anhydrase. I. Stop-flow kinetic studies on the native human isoenzymes B and C, J. Biol. Chem. 246 (1971) 2561–2573. http://www.ncbi.nlm.nih.gov/pubmed/4994926. (Accessed 2 December 2019).
- [41] P. Skehan, R. Storeng, D. Scudiero, A. Monks, J. Mcmahon, D. Vistica, J.T. Warren, H. Bokesch, S. Kenney, M.R. Boyd, New colorimetric cytotoxicity assay for anticancer-drug screening, J. Natl. Cancer Inst. 82 (1990) 1107–1112, https://doi.org/10.1093/jnci/82.13.1107.
- [42] R.M. Allam, A.M. Al-Abd, A. Khedr, O.A. Sharaf, S.M. Nofal, A.E. Khalifa, H.A. Mosli, A.B. Abdel-Naim, Fingolimod interrupts the cross talk between estrogen metabolism and sphingolipid metabolism within prostate cancer cells, Toxicol. Lett. 291 (2018) 77–85, https://doi.org/10.1016/ i.toxlet.2018.04.008.
- [43] N. Foudi, L. Louedec, T. Cachina, C. Brink, X. Norel, Selective cyclooxygenase-2 inhibition directly increases human vascular reactivity to norepinephrine during acute inflammation, Cardiovasc. Res. 81 (2009) 269–277, https:// doi.org/10.1093/cvr/cvn287.

- [44] V. Puigneró, J. Queralt, Effect of topically applied cyclooxygenase-2-selective inhibitors on arachidonic acid- and tetradecanoylphorbol acetate-induced dermal inflammation in the mouse, Inflammation 21 (1997) 431–442, https://doi.org/10.1023/A:1027370504822.
- [45] D. Wang, Y. Li, C. Zhang, X. Li, J. Yu, MiR-216a-3p inhibits colorectal cancer cell proliferation through direct targeting COX-2 and ALOX5, J. Cell. Biochem. 119 (2018) 1755—1766, https://doi.org/10.1002/jcb.26336.
- [46] T. Olszowski, I. Gutowska, I. Baranowska-Bosiacka, K. Piotrowska, J. Korbecki, M. Kurzawski, D. Chlubek, The effect of cadmium on COX-1 and COX-2 gene, protein expression, and enzymatic activity in THP-1 macrophages, Biol. Trace Elem. Res. 165 (2015) 135–144. https://doi.org/10.1007/s12011-015-0234-6.
- [47] S. Ivanov, S.Y. Liao, A. Ivanova, A. Danilkovitch-Miagkova, N. Tarasova, G. Weirich, M.J. Merrill, M.A. Proescholdt, E.H. Oldfield, J. Lee, J. Zavada, A. Waheed, W. Sly, M.I. Lerman, E.J. Stanbridge, Expression of hypoxia-inducible cell-surface transmembrane carbonic anhydrases in human cancer, Am. J. Pathol. 158 (2001) 905–919, https://doi.org/10.1016/S0002-9440(10)64038-2.
- [48] A. Blanco, G. Blanco, A. Blanco, G. Blanco, Apoptosis, in: Med. Biochem, Academic Press, 2017, pp. 791–796, https://doi.org/10.1016/B978-0-12-803550-4.00032-X.
- [49] N. Lounnas, C. Rosilio, M. Nebout, D. Mary, E. Griessinger, Z. Neffati, J. Chiche, H. Spits, T.J. Hagenbeek, V. Asnafi, S.A. Poulsen, C.T. Supuran, J.F. Peyron, V. Imbert, Pharmacological inhibition of carbonic anhydrase XII interferes with cell proliferation and induces cell apoptosis in T-cell lymphomas, Canc. Lett. 333 (2013) 76–88, https://doi.org/10.1016/j.canlet.2013.01.020.
- [50] M.L. Salem, N.M. Shoukry, W.K. Teleb, M.M. Abdel-Daim, M.A. Abdel-Rahman, In vitro and in vivo antitumor effects of the Egyptian scorpion Androctonus amoreuxi venom in an Ehrlich ascites tumor model, SpringerPlus 5 (2016) 570
- [51] S.S.W. Wong, O. Rasid, P. Laskaris, A. Fekkar, J.-M. Cavaillon, W.J. Steinbach, O. Ibrahim-Granet, Treatment of Cyclosporin A retains host defense against invasive pulmonary aspergillosis in a non-immunosuppressive murine model by preserving the myeloid cell population, Virulence 8 (2017) 1744–1752.
- [52] M.A. Bazm, L. Naseri, M. Khazaei, Methods OF inducing breast cancer IN animal models: a systematic review, World Canc. Res. J. 5 (2018).
- [53] N.Ö. Can, D. Osmaniye, S. Levent, B.N. Sağlık, B. Korkut, Ö. Atlı, Y. Özkay, Z.A. Kaplancıklı, Design, synthesis and biological assessment of new thiazolylhydrazine derivatives as selective and reversible hMAO-A inhibitors, Eur. J. Med. Chem. 144 (2018) 68–81, https://doi.org/10.1016/j.ejmech.2017.12.013.
- [54] D. Lagorce, O. Sperandio, H. Galons, M.A. Miteva, B.O. Villoutreix, FAF-Drugs2: free ADME/tox filtering tool to assist drug discovery and chemical biology projects, BMC Bioinf. 9 (2008), https://doi.org/10.1186/1471-2105-9-396.
- [55] http://fafdrugs4.mti.univ-paris-diderot.fr/ (accessed 2019-10-04), (n.d.).
- 56] http://preadmet.bmdrc.org/adme-prediction/ (accessed 2019-10-06), (n.d.).
- 57] http://www.openmolecules.org/datawarrior/ (accessed 2019-10-27), (n.d.).
- [58] C.A. Lipinski, F. Lombardo, B.W. Dominy, P.J. Feeney, Experimental and computational approaches to estimate solubility and permeability in drug discovery and development settings, Adv. Drug Deliv. Rev. 46 (2001) 3–26, https://doi.org/10.1016/S0169-409X(00)00129-0.
- [59] D.F. Veber, S.R. Johnson, H.-Y. Cheng, B.R. Smith, K.W. Ward, K.D. Kopple, Molecular properties that influence the oral bioavailability of drug candidates, J. Med. Chem. 45 (2002) 2615–2623, https://doi.org/10.1021/jm020017n.
- [60] W.J. Egan, K.M. Merz, J.J. Baldwin, Prediction of drug absorption using multivariate statistics, J. Med. Chem. 43 (2000) 3867–3877, https://doi.org/ 10.1021/jm000292e.
- [61] C. Abad-Zapatero, Ligand efficiency indices for effective drug discovery, Expet Opin. Drug Discov. 2 (2007) 469–488, https://doi.org/10.1517/ 17460441.2.4.469.
- [62] A.L. Hopkins, C.R. Groom, A. Alex, Ligand efficiency: a useful metric for lead selection, Drug Discov, Today Off. 9 (2004) 430–431, https://doi.org/10.1016/ S1359-6446(04)03069-7.
- [63] A.L. Hopkins, G.M. Keserü, P.D. Leeson, D.C. Rees, C.H. Reynolds, The role of ligand efficiency metrics in drug discovery, Nat. Rev. Drug Discov. 13 (2014) 105–121, https://doi.org/10.1038/nrd4163.
- [64] I. Wilkening, G. del Signore, C.P.R. Hackenberger, Synthesis of phosphonamidate peptides by Staudinger reactions of silylated phosphinic acids and esters, Chem. Commun. 47 (2011) 349–351, https://doi.org/10.1039/ COCC02472D.
- [65] V.R. Kamalraj, S. Senthil, P. Kannan, One-pot synthesis and the fluorescent behavior of 4-acetyl-5-methyl-1,2,3-triazole regioisomers, J. Mol. Struct. 892 (2008) 210–215, https://doi.org/10.1016/J.MOLSTRUC.2008.05.028.
- [66] H. Singh, J. Sindhu, J.M. Khurana, Efficient, green and regioselective synthesis of 1,4,5-trisubstituted-1,2,3-triazoles in ionic liquid [bmim]BF4 and in taskspecific basic ionic liquid [bmim]OH, J. Iran. Chem. Soc. 10 (2013) 883–888, https://doi.org/10.1007/s13738-013-0224-6.
- [67] H.-C. Wang, R.-S. Li, H.-R. Dong, H.-S. Dong, Note Synthesis of some new N-[4-acetyl-4,5-dihydro-5-(1-aryl-5-methyl-1H-1,2,3-triazol-4-yl)-5-methyl-1,3,4-thiadiazol-2-yl]acetamide derivatives, Indian J. Chem. 49B (2010) 521–525.
- [68] K. Ablajan, Synthesis and biological activity of some novel hydrazones containing triazole and thiazole, Chin. J. Org. Chem. 31 (2011) 724–727.
- [69] S.B. Vasamsetti, S. Karnewar, A.K. Kanugula, A.R. Thatipalli, J.M. Kumar, S. Kotamraju, Metformin inhibits monocyte-to-macrophage differentiation via AMPK-mediated inhibition of STAT3 activation: potential role in atherosclerosis, Diabetes 64 (2015) 2028–2041, https://doi.org/10.2337/db14-1225.
- [70] M.B. Labib, J.N. Philoppes, P.F. Lamie, E.R. Ahmed, Azole-hydrazone

- derivatives: design, synthesis, in vitro biological evaluation, dual EGFR/HER2 inhibitory activity, cell cycle analysis and molecular docking study as anticancer agents, Bioorg. Chem. 76 (2018) 67–80, https://doi.org/10.1016/j.bioorg.2017.10.016.
- [71] D. Hammond-McKibben, P. Lake, J. Zhang, N. Tart-Risher, R. Hugo, M. Weetall, A high-capacity quantitative mouse model of drug-mediated immunosuppression based on rejection of an allogeneic subcutaneous tumor, J. Pharmacol. Exp. Therapeut. 297 (2001) 1144–1151.
- [72] C. Shi, Q. Wang, X. Liao, H. Ge, G. Huo, L. Zhang, N. Chen, X. Zhai, Y. Hong, L. Wang, Y. Han, W. Xiao, Z. Wang, W. Shi, Y. Mao, J. Yu, G. Xia, Y. Liu, Discovery of 6-(2-(dimethylamino)ethyl)-N-(5-fluoro-4-(4-fluoro-1-isopropyl-2-methyl-1H-benzo[d]imidazole-6-yl)pyrimidin-2-yl)-5,6,7,8-tetrahydro-1,6-naphthyridin-2-amine as a highly potent cyclin-dependent kinase 4/6 inhibitor for treatment of cancer, Eur. J. Med. Chem. 178 (2019) 352–364, https://doi.org/10.1016/j.ejmech.2019.06.005.